Journal of Materials Chemistry B

ROYAL SOCIETY OF CHEMISTRY

REVIEW

View Article Online
View Journal | View Issue

Cite this: J. Mater. Chem. B, 2023, 11, 734

Antibacterial and antibiofilm mechanisms of carbon dots: a review

Meizhe Yu,[a] Peili Li,[b] Ruobing Huang,[a] Chunning Xu,[a] Shiyin Zhang,[a] Yanglei Wang,[a] Xuedong Gong[a] and Xiaodong Xing *[a]

Received 16th September 2022,
Accepted 12th December 2022

DOI: 10.1039/d2tb01977a

rsc.li/materials-b

Due to the increasing bacterial resistance to conventional antibiotics, developing safe and effective approaches to combat infections caused by bacteria and biofilms has become an urgent clinical problem. Recently, carbon dots (CDs) have received great attention as a promising alternative to conventional antimicrobial agents due to their excellent antimicrobial efficacy and biocompatibility. Although CDs have been widely used in the field of antibacterial applications, their antibacterial and antibiofilm mechanisms have not been systematically discussed. This review provides a systematic overview on the complicated mechanisms of antibacterial and antibiofilm CDs based on recent development.

1 Introduction

Drug-resistant bacterial infections have become a major threat to human health. At the site of bacterial infections, bacteria secrete large amounts of extracellular polymeric substances (EPSs) to form biofilms that can encase the bacteria and resist the penetration of antibacterial drugs such as antibiotics.[1–4] It is estimated that up to 80% of human bacterial infections are intertwined with biofilms.[5] Using traditional treatment strategies such as antibiotics, it is difficult to completely kill the bacteria within the biofilm and frequently requires large doses of antibiotics which tend to trigger bacterial resistance toward the antibiotics.[6,7] As antibiotic-resistant bacteria continue to emerge, many antibiotics are becoming less effective or ineffective in treating bacterial infections, which may lead to prolonged infections, more expense, and even increased mortality with common bacterial infections.[8,9] New kinds of antibiotics face issues such as high development costs and short duration of effectiveness, and cannot solve the root cause of bacterial resistance.[10] Therefore, it is of great practical significance to replace traditional antibiotics with new antimicrobial agents to treat bacterial infections.

Carbon dots (CDs) are a new type of zero-dimensional carbon nanomaterials, most of which are below 20 nm.[11] According to their structure and properties, CDs can be categorized into four classes: carbon quantum dots (CQDs), graphene quantum dots (GQDs), carbon nanodots (CNDs), and carbonized polymer dots (CPDs).[12] Since their first discovery in 2004,[13] CDs have been widely used in chemical and biological sensors,[14–16] cellular and biological imaging,[17,18] drug delivery and antimicrobial therapeutics[19–22] due to their chemical stability, excellent optical properties, outstanding biocompatibility and antimicrobial activity, and are better candidates for next generation nano antibacterial agents.[20,21] Other carbon-based nanomaterials including fullerenes, nanodiamonds, carbon nanotubes, graphene and their derivatives have also been widely discovered to exhibit excellent antibacterial activities and antibiofilm properties.[23,24] It is reported that the antibacterial mechanisms of nanomaterials are closely related to their physicochemical properties.[23] Due to the ultra-small size, CDs can more easily enter the interior of bacteria to exert antibacterial effects. For the antibiofilm mechanisms of carbon-based nanomaterials, the current reports are all about disrupting biofilms by killing bacteria in a biofilm matrix.[25,26] In contrast to them, CDs exhibit rich antibiofilm activity by hindering the adhesion process, disrupting community sensing, and killing bacteria.[27–29]

Although CDs have been widely used in antimicrobial applications, to the best of our knowledge, a comprehensive and systematic review of the antimicrobial and antibiofilm mechanisms of carbon dots is still lacking. Here, we will review the antimicrobial mechanisms of CDs in terms of their inhibitory and destructive effects on biofilms, physical damage to bacterial surfaces, oxidative damage, photothermal effects, effects on bacterial vital activities, and retention of drug molecule active structures. We hope this review will provide valuable guidance to the researchers who are exploring the antibacterial mechanism of CDs and promote the application in response to bacterial infections.

[a] School of Chemistry and Chemical Engineering, Nanjing University of Science and Technology, Nanjing, 210094, P. R. China. E-mail: xingxiaodong07@njust.edu.cn
[b] College of Chemistry and Materials Engineering, Anhui Science and Technology University, Bengbu, 233000, P. R. China

2 Antibacterial mechanisms of CDs

Many CDs have been reported to show the ability to kill bacteria. We summarize them in Table 1 and discuss their antibacterial mechanisms in terms of causing physical damage to bacterial structures, oxidative damage, photothermal effect, affecting bacterial cellular life activities, and retention of drug molecule active structures as shown in Scheme 1.

2.1 Causing physical damage to the bacterial structure

In contrast to eukaryotic cells, bacteria are prokaryotes that lack some organelles and a well-defined nucleus. The bacterial cell envelope consists of the cell wall and the cytoplasmic membrane. In Gram-positive bacteria, the cell walls contain a relatively thick and loose monolayer structure composed of peptidoglycan and phosphatidic acid.[30,31] Unlike Gram-positive bacteria, the cell walls of Gram-negative bacteria include two layers of peptidoglycan and an outer membrane containing lipoproteins, lipid bilayers and lipopolysaccharides.[30,31] The unique intensive and thin structure effectively reduces the penetration of macromolecules. It is reported that conventional antimicrobial agents can physically disrupt the integrity of cells to kill bacteria.[32–34] Similarly, carbon dots with antimicrobial properties can also cause physical damage to the bacterial cell envelope.

2.1.1 Effect of positive surface charges. The bacterial cell exhibits a negatively charged surface, which is mostly due to lipopolysaccharides and phosphatidic acid composed of both Gram-negative and Gram-positive cell envelopes.[21,35,36] Therefore, CDs with positive surface charges are prone to be adsorbed on the surface of bacterial cells by electrostatic interactions. The strength of the electrostatic interaction is mainly dependent on the magnitude of surface charge, which determines the bactericidal effect of CDs. When CDs accumulate on cell membranes, they can break the integrity of the cell membrane and cause cytoplasmic efflux, which in turn leads to the death of bacteria.

Jian *et al.*[37] synthesized positively charged carbon quantum dots (CQD_{Sps}) derived from spermidine, which exhibit effective antibacterial activity against non-drug-resistant *E. coli*, *S. aureus*, *P. aeruginosa* and *S. enterica*, as well as against methicillin-resistant *S. aureus*. The experimental results showed that CQD_{Sps} with small size (~6 nm in diameter) and high positive charge (ζ-potential ~ +45 mV) led to severe disruption of bacterial membranes, resulting in leakage of cellular components and eventually cell death. Zhao *et al.*[38] reported nitrogen–phosphorus co-doped carbon dots (N,P-CDs) prepared from glucose, polyethyleneimine, and phosphoric acid. Positively charged N,P-CDs can be easily attracted by negatively-charged bacteria, and attach onto bacteria cells. *S. aureus* without N,P-CDs treatment has clear edges and smooth cell walls. After treatment, the cell wall shrinks or even completely collapses and the leakage of cell contents increased indicating that N,P-CDs cause bacterial death by disrupting the bacterial cell wall and/or membrane. Lu *et al.*[39] demonstrated highly water-soluble carbon dots with good broad-spectrum antibacterial activity prepared from citric acid and curcumin. CDs destabilized the bacterial cell wall when it made contact with bacteria, causing roughness and atrophy of the bacterial surface. The bactericidal efficiency against Gram-negative bacteria (*E. coli* and *P. aeruginosa*) was up to 100% when the concentration of CDs reached 375 μg mL^{-1}. Cui *et al.*[40] prepared spermidine-*o*-phenylenediamine carbon quantum dots (Sps-Y-CDs, +51.20 mV) with a strong positive charge using a simple hydrothermal method. Methicillin-resistant *S. aureus* (MRSA) and multidrug-resistant *S. typhimurium* (MRST) were co-cultured with Sps-Y-CDs, showing in wrinkled surfaces and leakage of many intracellular contents. This suggested that Sps-Y-CDs with ultra-small size and strong positive charge achieved antibacterial effects by disrupting bacterial cell walls/membranes. Hao *et al.*[41] prepared positively charged carbon dots (PC-CQDs) with broad-spectrum antibacterial effects using citric acid, L-glutathione and polyethene polyamine as raw materials. The electrostatic effect promoted the adsorption of PC-CQDs by bacteria and enriched them on the bacterial surface. After treatment with PC-CQDs, many defects appeared on the surface of the originally intact and smooth cell wall/membrane, along with the leakage of intracellular contents. This indicated that PC-CQDs caused physical or mechanical damage to the bacterial cell wall/membrane, which induced the overall physiological dysfunction of the bacteria and even the leakage of cytoplasmic components, ultimately leading to death of the bacteria.

As shown in Fig. 1, our group prepared three similar carbon dots ($CD_{2.5w}$, CD_{1w}, and CD_{600}) using citric acid and PEI with different molecular weights as precursors.[29] CDs disrupted the bacterial cell membrane through electrostatic interaction, which eventually led to bacterial inactivation. The three CDs had the same surface groups, which endowed them with the same antibacterial mode. The different content of surface chemical groups, especially the ammonia/amine groups, made the three CDs exhibit different antibacterial activities. Among them, $CQD_{2.5w}$ had the most surface amino groups, which gave it the highest zeta potential value and the strongest electrostatic interaction with bacteria, possessing the best antimicrobial properties.

Generally, the increasing positive charge of carbon dots will improve their antibacterial activity, but the biocompatibility will significantly decrease, which is an important challenging problem to be solved.

2.1.2 Effect of hydrophobic interaction. A positively charged surface containing long-chain alkyl groups can bind to bacterial cell membranes and improve the attachment rate of carbon dots to the cell membrane, significantly improving the antibacterial properties of carbon dots. As shown in Fig. 2, Yang *et al.* developed quaternized CDs[42] containing long-chain alkyl groups. The CDs can selectively insert long-chain alkyl groups into the surface of Gram-positive bacteria, altering the charge balance on the bacterial surface, leading to the disruption of the bacterial surface and ultimately to bacterial inactivation. Similarly, Sviridova *et al.*[43] used quaternary ammonium salts containing long-chain alkyl groups for the modification of CDs.

Table 1 Summary of different CDs and their antibacterial effect

CDs label	Source (precursor)	Synthesis method	Bacteria	Antibacterial effect (μg mL^{-1})	Evaluation method	Antibacterial mechanism	Ref.
CQD_{Spds}	Spermidine	Pyrolysis	Broad spectrum	2–4	Standard dilution method	Electrostatic interaction	37
N,P-CDs	Glucose + PEI	Hydrothermal	Broad spectrum	*S. aureus* 7.5 *E. coli* 500	OD600	Electrostatic interaction	38
CDs	Citric acid + curcumin	Hydrothermal	Broad spectrum	375	OD600	Electrostatic interaction	39
Sps-Y-CDs	Spermidine + *O*-phenylenediamine	Hydrothermal	Broad spectrum	32–64	Standard dilution method	Electrostatic interaction	40
PC-CQDs	L-Glutathione + PEI + citric acid	Solvothermal	Broad spectrum	*S. aureus* 15 *E. coli* 480	Standard dilution method	Electrostatic interaction ROS Destruction of DNA structure	41
CD_{600}, CD_{1w}, $CD_{2.5w}$	Citric acid + PEI_{600}/PEI_{10000}/ PEI_{25000}	Hydrothermal	Broad spectrum	*S. aureus* 86.7/23.6/1.2 *E. coli* 326.6/ 154.2/47.8	Standard dilution method	Electrostatic interaction	29
CDs	Si-QAC + glycerol	Solvothermal	*S. aureus*	2500	Standard dilution method	Electrostatic interaction Hydrophobic interaction	42
CQDs	Ethylenediamine + citric acid + ADT-N + $(Alk)_3$	Hydrothermal	Broad spectrum	*S. aureus* 3.09 ± 1.10 *E. coli* 7.93 ± 0.17	OD600	Electrostatic interaction Hydrophobic interaction	43
C_{60}-GQD	C_{60}	Oxidation	*S. aureus*	200	Plate killing assays	Gaussian-curvature match	44
S-CQDs	Poly(sodium-4-styrene sulfonate)	Hydrothermal	*E. coli*	32	Plate killing assays	Size	46
N-CQDs	Polyvinylpyrrolidone	Hydrothermal	*E. coli*	32	Plate killing assays	Electrostatic interaction	46
s-CGCDs, m-CGCDs, l-CGCDs	Chlorhexidine gluconate	Hydrothermal	Broad spectrum	*S. aureus* 50/ 75/100 *E. coli* 75/ 100/100	OD540	Electrostatic interaction size DNA damage	45
CDs	Ampicillin	Hydrothermal	*S. aureus*	700	OD600	ROS	56
X/N-PGQDs, (X = Cl, Br, I)	Spermidine + hydrochloric acid/ hydrobromic acid/hydroiodic acid	Hydrothermal	Broad spectrum	*S. aureus* 0.05/0.05/1.9 *E. coli* 0.005/ 0.008/0.05	Standard dilution method	ROS	57
BrCND	HBr, acros organics	Combustion	Broad spectrum		Plate killing assays	ROS	58
CQDs	Citric acid + ethylenediamine	Hydrothermal	*S. aureus*		Plate killing assays	ROS	59
GQDs	Graphene	Chemical oxidation				ROS	60
N-CQDs	Bis-quaternary ammonium salt	Hydrothermal	Broad spectrum	AR *E. coli* 8 *E. coli* 8 MR *S. aureus* 4 *S. aureus* 2	OD600	Electrostatic interaction ROS Hinder bacterial metabolism	62
FA-CD	Folic acid	Solvothermal	*S. aureus*	16	Standard dilution method	ROS	63
CD_{Arg}	Arginine	Pyrolysis	Broad spectrum	*S. aureus* 62.5 *E. coli* 62.5	Standard dilution method	Electrostatic interaction ROS	20
CD_{Lys}	Lysine	Pyrolysis	Broad spectrum	*S. aureus* 16 *E. coli* 31.25	Standard dilution method	Electrostatic interaction ROS	20
N-GQDs	Nitro-coronene + BPEI (600, 1800, 10 000)	Hydrothermal	Broad spectrum	*S. aureus* 200 *E. coli* 200	Colony counting method	Photothermal effect	66
Fe-CDs	NaFeEDTA	Pyrolysis	Broad spectrum		Colony counting method	ROS Photothermal effect	67
CS/nHA/CD	Citric acid + glycine	Microwave	Broad spectrum		Colony counting method	Photothermal effect	68

Table 1 (*continued*)

CDs label	Source (precursor)	Synthesis method	Bacteria	Antibacterial effect ($\mu g\ mL^{-1}$)	Evaluation method	Antibacterial mechanism	Ref.
PCQDs	Papaya leaf	Hydrothermal	Broad spectrum	250	Colony counting method	Photothermal effect ROS	69
CPDs	3,4-Dihydroxybenzaldehyde functionalized chitosan (DFC)	Solvothermal	Broad spectrum	*S. aureus* 31.5 *E. coli* 125	Standard dilution method	Electrostatic interaction Photothermal effect	70
CDs	Vitamin C	Microwave	Broad spectrum	*S. aureus* 100 *B. subtilis* 50 *E. coli* 75	OD600	Destruction of DNA structure	75
qCQDs	Glucose + Dimethyl diallyl ammonium chloride	Solvothermal	Broad spectrum	*S. epidermidis* 12 *S. aureus* 25 MR *S. aureus* 25 *E. faecalis* 25 *E. coli* 50 *P. aeruginosa* 50	Standard dilution method	Influence on protein activity	76
ACDs	Artemisia argyi leaves	Combustion	*E. coli*	50000	OD600	Altering the enzymatic secondary structure	77
SCD	Spermine	Pyrolysis	*E. coli*		Colony counting method	Programmed death	81
CDs-Kan	Kanamycin sulfate	Hydrothermal	Broad spectrum	8	Colony counting method	Retention of antibacterial active structures	83
LCDs	Levofloxacin	Hydrothermal	Broad spectrum	*S. aureus* 125 *E. coli* 125 *S. marcescens* 125 MR *S. aureus* 250 *P. aeruginosa* 250 *S. epidermidis* 500 *E. faecalis* 500	OD600	Retention of antibacterial active structures Electrostatic interaction ROS	84
CNDs	Metronidazole	Hydrothermal	*P. gingivalis*	1.25	OD600	Retention of antibacterial active structures	82
CQD_{Gent}	Gentamicin sulfate	Pyrolysis	Broad spectrum	*S. aureus* 1.59 *E. coli* 203.4	Standard dilution method	Retention of antibacterial active structures electrostatic interaction ROS	21

The antibacterial results showed that the change in alkyl chains led to a significant increase in the antibacterial effect of CDs against *S. aureus* and *E. coli*. This was attributed to the fact that the introduction of hydrophobic alkyl chains enhanced the affinity of CDs for cell membranes, leading to the aggregation of CDs and disruption of cell membrane equilibrium, while the hydrophobicity of alkyl chains promoted the penetration of CDs into the hydrophobic lipid layer of cell membranes, thus causing further damage and disruption to them.

Similar to the effect of positive charge, the increase of hydrophobicity will lead to an increase in the toxicity of CDs, and may cause the aggregation of nano particles, which is disadvantageous to the practical application of CDs.

2.1.3 Effect of particle morphology and size. Besides electrostatic interactions and hydrophobic interactions, there are other modes of action that can lead to the disruption of bacterial cell membranes. The size of CDs obviously had an effect on their antibacterial activity.

The graphene quantum dots (C_{60}-GQD)[44] prepared by Hui *et al.* were effective in killing *S. aureus*, but had no antibacterial activity against *B. subtilis*, *E. coli* or *P. aeruginosa* (Fig. 3). Their antibacterial activity may be related to the ability of C_{60}-GQD to disrupt the bacterial cell envelope. The surface Gaussian curvature match between a GQD and a target bacterium may play a pivotal role in determining whether the GQD can be associated with the cell surface of the target bacterium, to initiate the subsequent bactericidal envelope destabilization processes. It can be suggested that the curvature match between the C_{60}-GQD and the bacterial surface led to the disruption of the bacterial cell envelope, which in turn led to the death of the bacteria. Sun *et al.*[45] used a biguanide antibacterial drug (chlorhexidine gluconate) as a raw material to prepare carbon

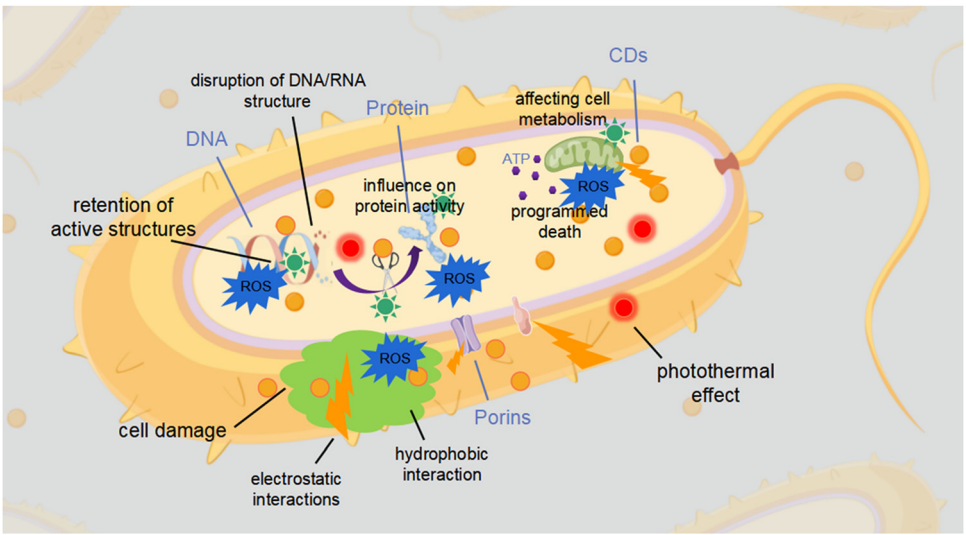

Scheme 1 Antibacterial mechanisms of CDs.

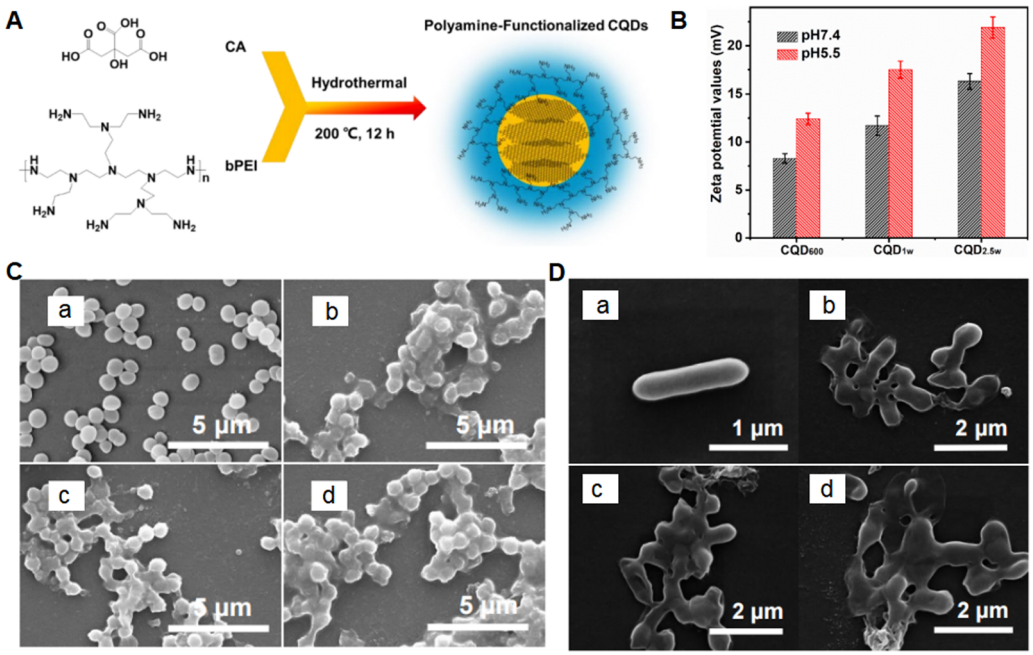

Fig. 1 (A) Synthetic route of the polyamine-functionalized CQDs. (B) Zeta potentials of CQDs in pH 7.4 and pH 5.5 PBS. (C and D) SEM images of *S. aureus* and *E. coli*. (a and d) Refer to untreated cells (control), CQD_{600}, CQD_{1w} and $CQD_{2.5w}$ (250 μg mL^{-1}). Reprinted with permission.[29]

dots (CGCD). The abundant amino/imine functional groups on the surface of CGCD were able to interact electrostatically with the anionic sites of lipid phosphates on the cell membrane. This caused an inhomogeneous surface charge on the cell membrane surface, leading to leakage of low molecular weight compounds such as potassium ions from the cell and progressively disrupting the membrane integrity. In addition, they found a significant effect of the particle size of CGCD on its antimicrobial activity. Comparing with other sizes, CGCD with a smaller size had significantly enhanced antibacterial activity which may be due to the differences in cellular uptake and distribution of CDs in the plasma membrane. Travlou *et al.*[46] prepared sulfur- and nitrogen-doped carbon quantum dots (S-CQDs and N-CQDs) using poly(sodium 4-styrenesulfonate) or polyvinylpyrrolidone respectively. S-CQDs and N-CQDs exhibited obvious inhibitory effects on the growth of Gram-positive (*B. subtilis*) and Gram-negative (*E. coli*) bacteria. The surface chemistry and size of the CDs were the main factors affecting their antibacterial activity.

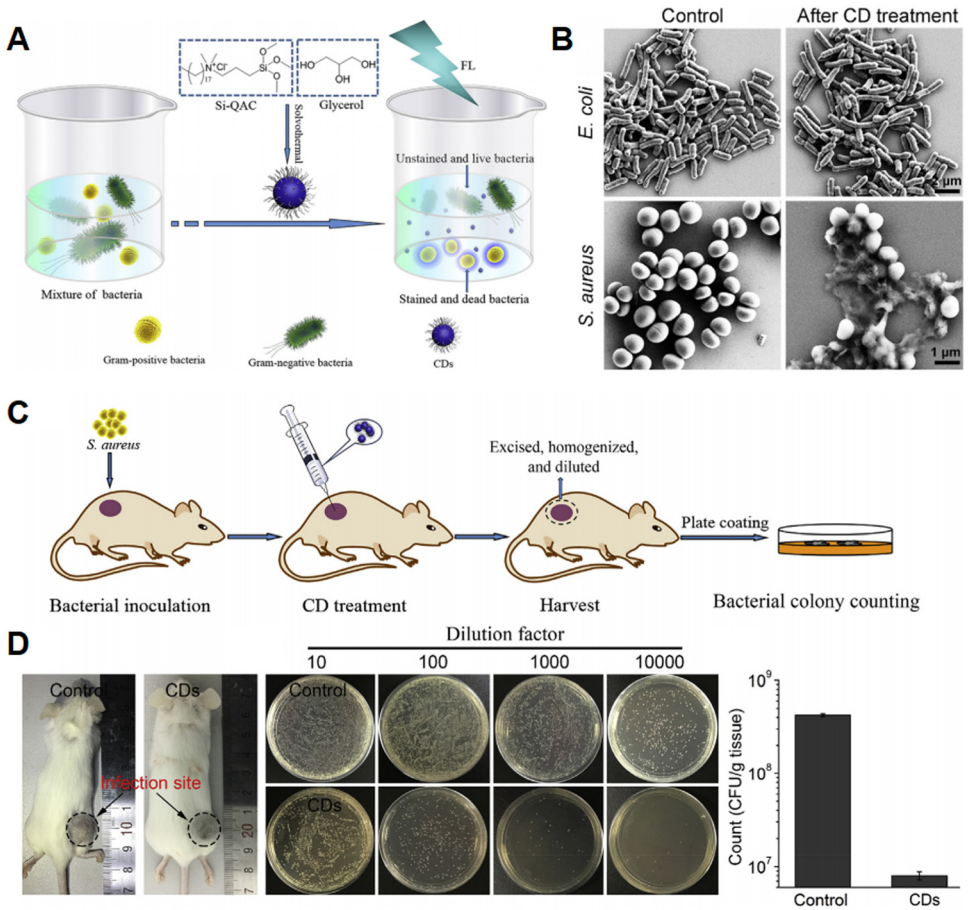

Fig. 2 (A) Schematic illustrating the preparation of quaternized CDs and their application for selective imaging and killing of Gram-positive bacteria. (B) SEM images of *E. coli* and *S. aureus* cells without (left) or with (right) the treatment of CDs (30 mg mL^{-1}) for 2.5 h. (C and D) *In vivo* antibacterial performance of CDs. Reprinted with permission.[42]

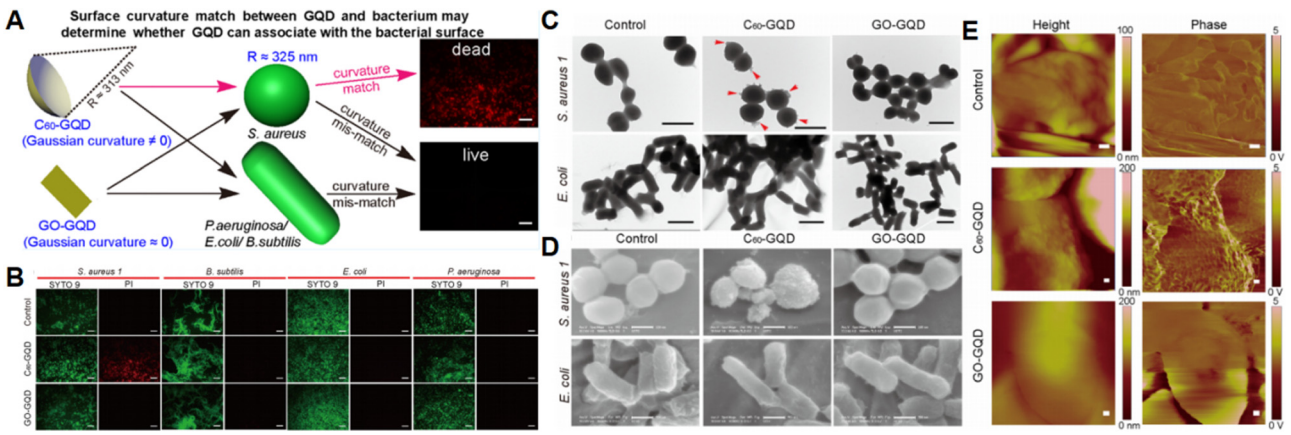

Fig. 3 (A) Schematic illustrating the preparation of C_{60}-GQD and their application for selective killing of Gram-positive bacteria. (B) Fluorescence microscopy images and (C and D) SEM image of bacteria after C_{60}-GQD (400 μg mL^{-1}) treatment. (E) AFM height (left) and tapping phase (right) images of *S. aureus* cells with and without C_{60}-GQD treatment. Reprinted with permission.[44]

Because of the protonation of nitrogen-containing functional groups on the surface, electrostatic interactions between positively charged N-CQDs and negatively charged cell membranes were the main source of their antimicrobial activity. The surface of S-CQDs was

mainly negatively charged due to the dissociation of sulfonic acid/carboxylate and sulfate groups, showing a size dependence on bacterial growth.

2.2 Oxidative damage

Another common toxic effect caused by CDs is oxidative damage. Normally, reactive oxygen species (ROS) in bacterial cells are regulated by their oxidoreductase system, maintaining a dynamic balance at a relatively normal level. When the level of ROS increased, it can cause some irreversible damage to the bacterial cells, such as the destruction of cell membrane, mitochondrial membrane and other membrane structures, oxidative damage to proteins, lipids, *etc.*, and the breakage of DNA strands.[23,47–55]

Gao *et al.* synthesized novel carbon dots (CDs) by a one-pot hydrothermal method using ampicillin.[56] The CDs showed good antibacterial activity against *S. aureus* and *L. monocytogenes* even at low concentrations. Their antibacterial mechanism originated from the fact that CDs were able to produce ROS under visible light irradiation, which acts on the surface of bacteria, disrupting the cell membrane and causing cytoplasmic leakage. Visible light activated halogen/nitrogen co-doped polymeric graphene quantum dots [X/N-PGQDs, (X = Cl, Br, I)][57] were developed by Huang *et al.* After 1 min of irradiation with LED light, the inhibitory effect of X/N-PGQDs on the different bacterial strains tested was significantly increased. The MIC values of X/N-PGQDs under LED light irradiation were 100-fold lower compared to those in a dark environment. This was due to the production of ROS, which induced oxidative stress in bacteria, thus disrupting the integrity of cell membranes and leading to cell death. Knoblauch *et al.*[58] synthesized brominated carbon nanodots (BrCNDs) as photosensitizers. Under UV light (365 nm) irradiation, BrCNDs produced ROS in both oxygen-enriched and oxygen-deficient solutions, which subsequently caused oxidative damage to nearby bacterial cell membranes, leading to inhibition of bacterial activity and even death. Tang *et al.*[59] synthesized a metal-free heterojunction CQDs/g-C_3N_4 photocatalyst. The photocatalytic inactivation of *S. aureus* was significantly enhanced *in vitro* compared to pure g-C_3N_4. The interaction between CQDs and g-C_3N_4 significantly promoted the separation of photogenerated electron–hole pairs and charge-transfer properties, which increased the production of ROS. The rapid increase of intracellular ROS levels caused the cell membrane to be disrupted, eventually leading to death of bacteria. Chong *et al.*[60] prepared graphene quantum dots (GQDs) using a chemical oxidation and cutting method. Upon exposure to blue light, GQDs reduced cell viability by increasing intracellular ROS levels. They confirmed that light-induced ROS formation originated from electron–hole pairs and, more importantly, revealed that singlet oxygen was generated by light-excited GQDs *via* energy transfer and electron transfer pathways. Furthermore, under photoexcitation, GQDs accelerated the oxidation of non-enzymatic antioxidants and promoted lipid peroxidation, which promoted the phototoxicity of GQDs. Walia *et al.*[61] synthesized a series of fluorescent carbon dots (CDs) using carbohydrates, cysteine and o-phenylenediamine as the carbon and nitrogen sources, respectively. Antimicrobial studies showed that the OPD-based CDs were more effective against *E. coli* with an IC_{50} value of 200 μg mL^{-1} compared to the Cys-based CDs. The antimicrobial activity of the developed CDs involved three simultaneous steps, namely: cell membrane rupture through lipid peroxidation induced by oxidative stress; DNA degradation induced by oxidative stress after entry of the CDs into the bacterial cells; and release of cytoplasmic contents. Wang *et al.*[62] obtained nitrogen-doped carbon quantum dots (N-CQDs) using

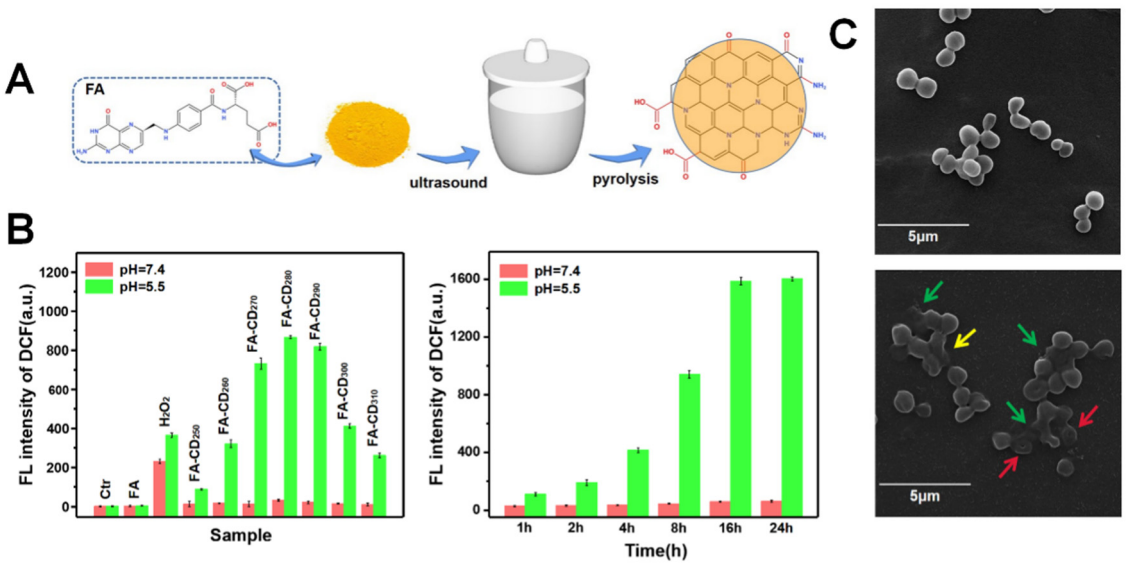

Fig. 4 (A) Schematic representation of the synthesis of FA-CDs. (B) Fluorescence intensity of intracellular DCF^+ inside *S. aureus*. (C) SEM image of normal *S. aureus* (control) and *S. aureus* cocultivated with FA-CD_{280} (1 mg mL^{-1}) for 4 h. Reprinted with permission.[63]

biquaternary ammonium salts as precursors, which interacted with bacterial cell membranes *via* electrostatic interaction, leading to severe damage and increased permeability of the cell membrane. This further facilitated the penetration of N-CQDs into the cell and induced the production of ROS.

As shown in Fig. 4, folic acid carbon dots (FA-CDs) prepared by our group using folic acid as a precursor, had selective antibacterial activity against *S. aureus*.[63] They were able to accumulate on the cytoplasmic membrane of *S. aureus* and exhibit excellent oxidase-like and peroxidase-like activities in the acidic environment of the infection site, gradually increasing the intracellular ROS level. At the same time, they can inhibit the activity of superoxide in *S. aureus* cells, leading to a diminished ability of the bacteria to scavenge excess ROS. These two aspects, together, led to the disruption of ROS homeostasis in the bacterial organism, rendering various proteins inactive, degrading nucleic acids, disrupting the integrity of cell membranes, and ultimately leading to death of the bacteria. In addition, we prepared arginine carbon dots (CD_{Arg}) and lysine carbon dots (CD_{Lys})[20] using arginine and lysine as precursors, respectively. These two carbon dots had superb cell selectivity and not only had excellent antibacterial and biofilm inhibition effects, but also promoted mammalian cell growth and wound healing, breaking the conventional notion of antibacterial agent selectivity. Their antimicrobial activity was attributed to the combined effect of positively charged surfaces and ROS production, which disrupted the integrity of cell membranes and led to death of the bacteria.

So, intracellular ROS plays an extremely important role. Researchers can regulate the level of ROS in bacteria and introduce environment responsive mechanisms, which will improve the performance of CDs and bring smart antibacterial functions.

2.3 Photothermal effect

In addition to the destruction of cell membrane structures by physical action and the inducing increased ROS causing oxidative damage, photothermal therapy (PTT) is a common way to kill bacteria for CDs. CDs with photothermal conversion properties can increase the local temperature under near-infrared light excitation, causing DNA damage and protein denaturation of bacteria. This modality has multiple advantages, such as minimally invasive, low systemic toxicity and excellent controllability.[64,65]

Geng *et al.*[66] prepared highly graphitic N-GQDs using nitrocoronene and branched polyethylenimine as precursors. The N-GQDs had efficient photothermal conversion properties, and the graphitic N sites could act as paramagnetic F centers to mediate efficient NIR absorption and photothermal conversion for photothermal antimicrobial therapy. For both MDR bacteria (MRSA) and non-MDR bacteria (*S. aureus* and *E. coli*), N-GQDs showed broad-spectrum antimicrobial activity and biofilm elimination under NIR-II laser to accelerate infected wound healing. N-GQDs without laser irradiation had no significant antibacterial effect, and the survival rate of MRSA treated with N-GQDs (200 mg mL^{-1}) under NIR laser irradiation was less than 3%. These results suggested that N-GQDs with strong NIR absorption can convert laser energy into thermal energy to kill bacteria. Liu *et al.*[67] prepared iron-doped carbon dots (Fe-CDs) by a simple one-pot pyrolysis method which had excellent photothermal conversion and photo-enhanced enzyme-like properties, and could be used for synergistic and efficient antimicrobial therapy and wound healing. Fe-CDs showed excellent photothermal conversion performance (η = 35.11%) under near-infrared laser irradiation. The photothermal effect produced by Fe-CDs not only induced bacterial death without causing damage to normal tissues, but also improved the catalytic efficiency of Fe-CDs. *In vitro* antibacterial experiments showed that the combination of POD-like activity and local mild heat resulted in 99.68% and 99.85% inhibition of Fe-CDs against *S. aureus* and *E. coli*, respectively. Lu *et al.*[68] prepared a novel CDs-doped chitosan/nanohydroxyapatite (CS/nHA/CD) scaffold. It exhibited significant antibacterial properties against clinically collected *S. aureus* and *E. coli*, and the antibacterial activity was further enhanced by NIR irradiation. The change in antimicrobial activity was attributed to the fact that CDs, as photosensitizers, were able to significantly increase the local temperature under NIR irradiation. When the temperature exceeded 50 °C, it caused irreversible DNA damage and protein denaturation in bacterial cells. Panda *et al.*[69] prepared a NIR-excited antimicrobial hydrogel by encapsulating papaya-derived carbon dots (PCQDs) in a polyethyleneimine–melamine hydrogel. PCQDs can precisely produce photothermal effects and ROS under NIR excitation which led to significant antimicrobial activity against both Gram-positive and Gram-negative bacteria.

Our group prepared carbonized polymeric dots (CPDs)[70] with photothermal enhanced antibacterial effects by using catechol-modified chitosan polymer as the precursor (Fig. 5). CPDs had a rapid and efficient bactericidal effect on *S. aureus* and 500 μg mL^{-1} CPDs were able to kill more than 98%. Compared with that of *S. aureus*, it finally killed only about 60% of *E. coli* even at a concentration of 2.5 mg mL^{-1}. Under NIR light irradiation, the bactericidal effect of CPDs on *E. coli* was greatly improved reaching about 95%. This is because under NIR light irradiation, CPDs with photothermal conversion ability increased the ambient temperature. It is well known that the enzymatic activity of bacteria changed when they were exposed to an environment higher than 45 °C, in which case they were more easily killed.

PTT is a promising strategy to kill bacteria, particularly for dealing with multidrug-resistant bacteria infection. Researchers can make full use of the advantages of PTT to incorporate it in other antibacterial approaches to improve killing efficiency and reduce side effects.

2.4 Affecting bacterial cellular life activities

After entry into the bacterial cells, CDs can bind to DNA/RNA, proteins, or other important cellular components, affecting the normal life activities of bacterial cells and eventually leading to death of the bacteria.

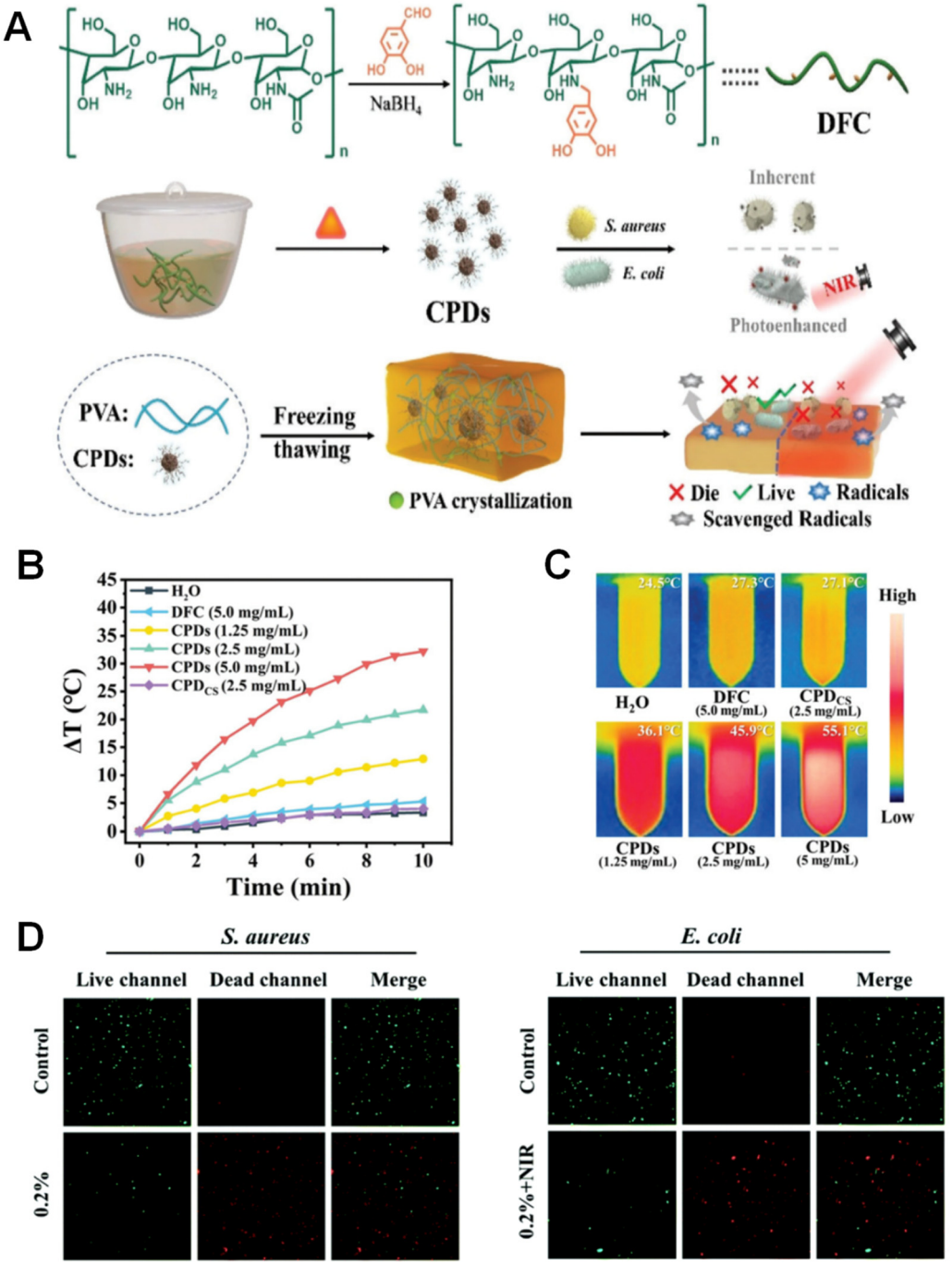

Fig. 5 (A) Synthetic route of PVA@CPDs hydrogel and its application. (B and C) Photothermal effect of CPDs. (D) *In vitro* antibacterial activity of hydrogels. Reprinted with permission.[70]

2.4.1 Affecting the structure and function of DNA/RNA. DNA can fold into ordered inter- and intramolecular secondary structures and show various conformations. Their stability is important for DNA replication, repair, transcription, gene expression and mitosis.[71–73] CDs may interact or adsorb with DNA or RNA through electrostatic attraction, nucleobase interaction and hydrophobic interaction to disrupt their conformations, thus causing some errors in gene delivery and inhibiting bacterial growth.[37,74]

As shown in Fig. 6, Li *et al.* used an electrochemical approach to prepare low toxicity and degradable carbon dots (CDs) from vitamin C.[75] The CDs with spectral antibacterial and antifungal activities achieved excellent bactericidal effects even at very low concentrations. It can disrupt bacterial walls and enter bacteria by diffusion. The authors investigated the binding interactions of CDs on DNA and RNA in bacteria by dynamic light scattering (DLS), circular dichroism spectroscopy and gel electrophoresis. The results showed that CDs can bind

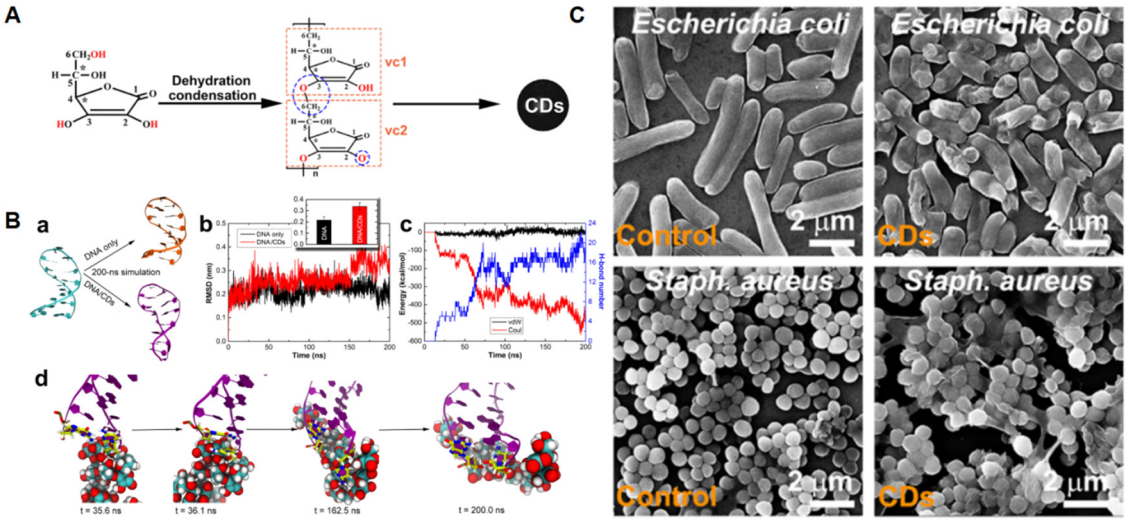

Fig. 6 (A) Simulated formation process of CDs. (B) (a) Original (cyan) and final configurations of DNA hairpin in the control (orange) and added CDs (purple) simulations; (b) time evolutions of the root mean square deviation (RMSD) of DNA heavy atoms in the control and added CD simulations. The embedded figure represents the average RMSD values for these two simulations over the last 40 ns data; (c) the direct nonbonded interaction energies, including vdW (black curve) and Coulomb (red curve) interaction energies, and hydrogen bond number (H-bond, blue curve) formed between CDs and DNA hairpin as a function of simulation time; (d) some representative configurations were taken from some key time points to show the terminal base pair denaturation process. The terminal base pair was shown with sticks, where red, yellow, blue, and tan sticks represent oxygen, carbon, nitrogen, and phosphorus atoms, respectively. The purple ribbon indicates the DNA hairpin. The cyan, red, and white spheres were carbon, oxygen, and hydrogen atoms of the CDs. (C) The SEM images of *S. aureus* (Gram-positive) and *E. coli* (Gram-negative) after incubation without and with CDs at 60 μg mL^{-1} for 12 h. Reprinted with permission.[75]

to DNA and RNA and fungi through non-covalent bonds, change the secondary structure of DNA and RNA, and then affect the genetic processes of bacteria and fungi, ultimately killing them. Hao *et al.* prepared PC-CQDs that were able to disrupt the membrane structure of bacteria by physical action and cause cytoplasmic exocytosis.[41] Meanwhile, they used FAM-labeled random sequence DNA to monitor the possible uptake of genes on PC-CQDs and performed circular dichroism spectroscopy analysis of the interaction between DNA and PC-CQDs. The results showed that PC-CQDs can absorb and interact with DNA upon entry into cells, leading to conformational changes that may eventually lead to bacterial cellular dysfunction.

2.4.2 Influence on protein activity. Ribosomal proteins are intracellular components, mainly related to ribosomes, involved in the biological process of protein translation, and their molecular functions are mainly focused on the structural components of ribosomes and RNA/rRNA binding. The molecular functions of proteins associated with the citrate cycle are mainly focused on the activities of various enzymes, including aconitate hydratase, isocitrate dehydrogenase ($NADP^+$), oxyglutamate dehydrogenase (succinyl-transferring), oxidoreductases and electron carriers, *etc.* Zhao *et al.* synthesized quaternized carbon quantum dots (qCQDs) with broad-spectrum antibacterial activity by a simple one-pot method with dimethyldiallyl ammonium chloride and glucose as precursors.[76] qCQDs showed excellent antibacterial activity against both Gram-positive and Gram-negative bacteria. To elucidate the antibacterial mechanism of qCQDs against bacteria, the authors performed quantitative proteomics studies based on tandem mass tagging (TMT) using *S. aureus* and *E. coli*, respectively, to analyze the protein changes of bacteria before and after qCQDs treatment. Meanwhile, gene set enrichment analysis was performed to further analyze the genes of differentially expressed proteins in the Kyoto Encyclopedia of Genes and Genomes pathway, and real-time quantitative PCR was used to verify the expression of relevant protein genes. The results showed that their antibacterial activity was mainly related to the changes in protein activity of bacteria before and after treatment. That is, qCQDs mainly acted on ribosomal proteins of Gram-positive bacteria to interfere and disrupt bacterial protein synthesis; for Gram-negative bacteria, qCQDs mainly interfered with their cellular respiration by down-regulating essential proteins in the citrate cycle, further disrupting a variety of relevant metabolic pathways in bacterial cells.

Gram-negative bacteria have a unique bacterial outer membrane composed of phospholipids and lipopolysaccharides. Among them, lipid A is an important component of lipopolysaccharide, and its biosynthesis is mediated by a zinc metalloenzyme, UDP-3-*O*-(acyl)-*N*-acetylglucosamine deacylase (LPXC). As shown in Fig. 7, Wang *et al.*[77] prepared carbon dots from *Artemisia argyi* leaves (ACDs), which exhibited selective killing ability against Gram-negative bacteria. The experimental results showed that ACD could affect the structure of LPXC and inhibit the activity of cell wall-related enzymes in Gram-negative bacteria, disrupting the cell wall and leading to bacterial inactivation.

2.4.3 Affecting cell metabolism. Energy metabolism is a fundamental feature of bacterial life activity and is the basis for bacterial growth and reproduction. Wang *et al.*[62] prepared

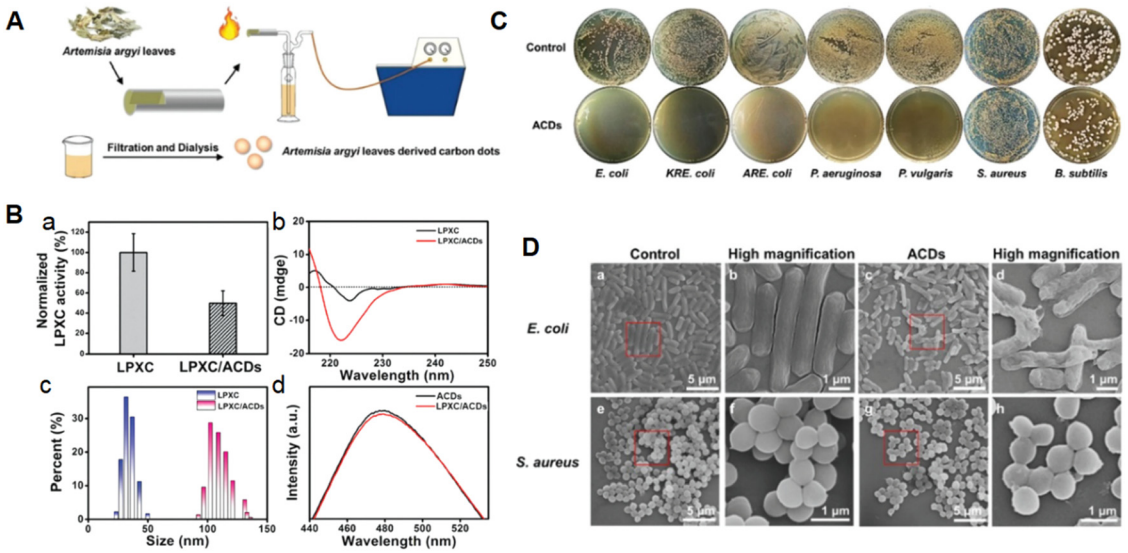

Fig. 7 (A) Synthesis process diagram of ACDs. (B) (a) The activity of free LPXC and LPXC/ACDs; (b) circular dichroism spectra of free LPXC and LPXC/ACDs; (c) size distribution of free LPXC and LPXC/ACDs; (d) PL spectra of ACDs and LPXC/ACDs excited at 400 nm. (C) Photographs of LB agar plates of *E. coli*, KRE *E. coli*, ARE *E. coli*, *P. aeruginosa*, *P. vulgaris*, *S. aureus* and *B. subtilis* incubated with or without ACDs (150 mg mL^{-1}). (D) SEM images of *E. coli* treated without ACDs and with ACDs, and *S. aureus* treated without ACDs and with ACDs. Reprinted with permission.[77]

nitrogen-doped carbon quantum dots (N-CQDs) using biquaternary ammonium salts as precursors. The intracellular ATP levels were measured using an ATP assay kit and luminescence intensity values to assess the effect of N-CQDs on bacterial metabolism. The results showed that the intracellular ATP levels gradually decreased with increasing N-CQD concentrations, indicating that it did hinder bacterial metabolism to some extent.

2.4.4 Programmed death. Under environmental stress, stressful adaptations occur after bacteria are induced, leading to functional differentiation, death or dormancy of cells. Programmed death, a cell death phenomenon activated by the cell's own programmed suicide mechanism, is a fundamental biological process necessary for bacteria to maintain individual structural stability, functional homeostasis and growth and development.[78,79] Among them, endogenous ROS levels are one of the most important apoptosis inducing triggers and apoptotic effector molecules.[80] Bing *et al.*[81] prepared three different carbon dots, including positively charged spermine C-dot (SCD), negatively charged candle-soot C-dot (CCD) and uncharged glucose C-dot (GCD), and systematically investigated the interaction of *E. coli* with the three typical CDs. The results showed that the production of ROS induced by the three C-dots differed significantly, which may lead to different antibacterial abilities. After treatment with negatively charged CCDs and positively charged SCDs, an apoptotic program was observed in *E. coli*, inducing programmed death. The uncharged GCD hardly had any effect on *E. coli*.

2.5 Retention of drug molecules active structures

Several studies have found that CDs retain some of the properties of their precursors. Based on these properties, researchers have developed CDs with excellent antimicrobial functions by selecting antimicrobial drugs as precursors. They can retain the antibacterial activity of the raw material and possess the properties of nanomaterials.[16,82]

Luo *et al.*[83] reported carbon dots (CDs-Kan) prepared with kanamycin sulfate. Its surface retained aminoglycosyl and aminocyclic alcohol groups, which can increase the permeability of bacterial cell membranes. The strength of the cell wall of *E. coli* treated with CDs-Kan decreased, the cell wall thinned, vesicles formed, and intracellular material leaked, eventually leading to cell death. Levofloxacin was one of the commonly used clinical nootropics with broad spectrum and strong antibacterial effects but its application was limited by drug resistance. Wu *et al.*[84] used a simple one-pot hydrothermal method to synthesize levofloxacin-based carbon dots (LCDs) with enhanced antibacterial activity and low drug resistance. The results indicated that LCDs possessed effective antibacterial properties by preserving the active groups of the levofloxacin. In addition, LCDs had a dual antimicrobial mode based on the positive surface charge and the production of reactive oxygen species. Liu *et al.*[82] synthesized carbon nanodots (CNDs) with selective antibacterial activity using metronidazole as the raw material. Metronidazole is a broad-spectrum antibiotic targeting specific anaerobic bacteria, and scholars generally believe that its mechanism of action is related to $-NO_2$ in the structure of metronidazole. The experimental results showed that CNDs had a high inhibitory effect on specialized anaerobic bacteria such as *P. gingivalis*, but could not inhibit the activity of facultative anaerobes, obligate aerobes, exhibiting the same selective antibacterial properties as metronidazole. The physicochemical property characterization showed that the pharmacodynamic functional group $-NO_2$ was still present in the structure of CNDs. Unlike other CDs that achieve bacterial inhibition by surface charge, the inhibition mechanism of

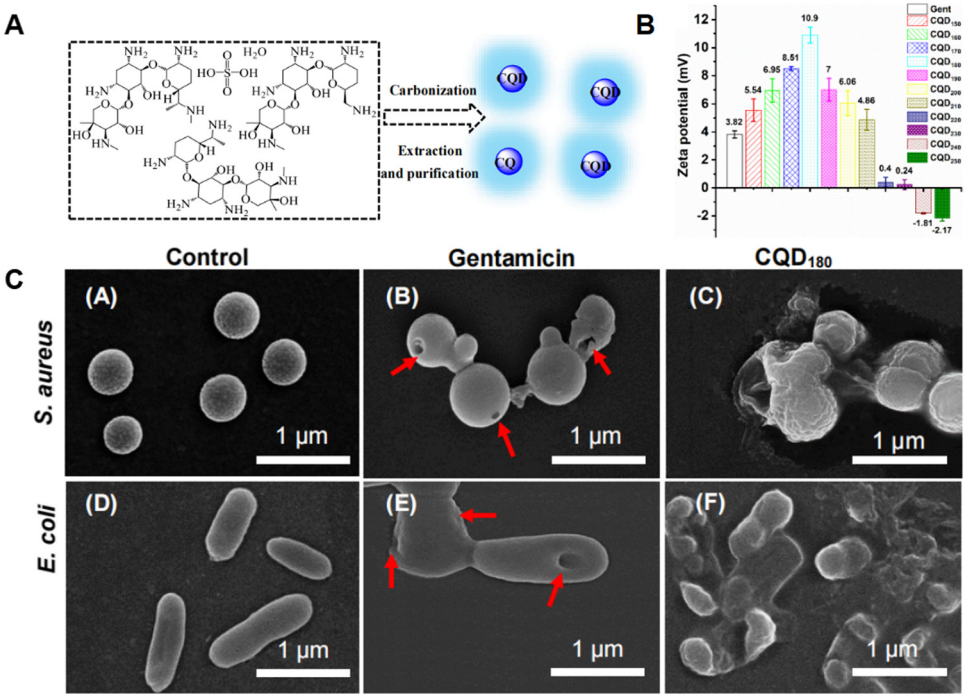

Fig. 8 (A) Process of preparing CQD_{Gent}. (B) Zeta potential of gentamicin and CQD_{Gent}. (C) SEM images of bacteria. Reprinted with permission.[21]

CNDs was mainly related to the retention of the pharmacodynamic functional group $-NO_2$, which was consistent with that of metronidazole. Bacteria had different cell structures, and the nitro on the surface of CNDs can be reduced to hydroxylamine only in specialized anaerobic bacteria, which further disrupted DNA synthesis and inhibited the activity of specialized anaerobic bacteria.

Our group prepared carbon quantum dots (CQD_{Gent}) using gentamicin sulfate as a precursor (Fig. 8).[21] Characterization and analysis of the structure of CQD_{Gent} confirmed that it retained some of the antibacterial active groups of gentamicin, which was the main source of their antibacterial activity. At the same time, it had multiple antibacterial modes. Due to the residual amino protonation on the surface, the CQD_{Gent} surface exhibited a positive charge in acidic solutions and can have electrostatic interactions with bacterial cell membranes. CQD_{Gent} was able to induce ROS production in bacterial cells. The ROS level induced by 6 μg mL^{-1} CQD_{Gent} was even higher than that produced by the positive control (H_2O_2, 1 mM), which had a strong oxidative capacity and can effectively inhibit bacterial growth. The morphology of untreated *S. aureus* and *E. coli* was intact, and the bacterial cell surface was smooth and undamaged. After CQD_{Gent} treatment, the bacterial cell membrane ruptured significantly, intracellular contents flowed out of the bacteria, and the bacteria were inactivated.

Above all, compared to small molecule antimicrobial drugs, CDs can enter the interior of biofilms more easily and may also possess other antibacterial modes. In this way, they can inhibit and kill bacteria more rapidly and more extensively, while reducing the risk of bacterial resistance.

3 Antibiofilm mechanisms of CDs

Bacterial biofilms are the membrane-like substances when bacteria secrete large amounts of extracellular polymeric substances (EPS) to adapt to the surrounding microenvironment and wrap the bacterium itself in them.[4,85] Many Gram-positive and Gram-negative bacteria, such as *S. aureus*, *P. aeruginosa*, *B. subtilis*, and *P. gingivalis*, can form biofilms.[25] The growth of bacterial biofilms begins with the formation of substrate surfaces. Once bacteria adhere to these surfaces, they will utilize available nutrients to multiply.[86] The adhesion of bacteria to surfaces is primarily controlled by bacterial life behaviors.[87] This is the result of the expression of some genes that are responsible for the production of surface proteins like porins. Porins contribute to the transport of polysaccharides, which are used to form the EPS layer. As biofilms mature, bacteria also begin to communicate among themselves by secreting self-induced signals,[88] *i.e.*, quorum sensing. Biofilms are divided into ''communities'', each of which is responsible for a specific task, so this communication is essential. Currently, the common clinical approach to prevent biofilm infections is to use very high doses of antibiotics such as gentamicin, tobramycin and ciprofloxacin in the early stages of biofilm formation.[89] However, biofilm can resist the penetration of antibiotics and reduce the effect of drugs on the bacteria encapsulated in it, and is an important cause of treatment failure and recurrent infections. Considering the biofilm's protective effect on the pathogenic bacteria hidden in it, inhibition of biofilm formation and elimination of mature established biofilm was an effective way to avoid the worsening of infection. We

Table 2 Summary of different CDs and their antibiofilm effect

CDs label	Source (precursor)	Synthesis method	Antibiofilm type	Bacteria	Antibiofilm effect	Concentration ($\mu g\ mL^{-1}$)	Evaluation method	Antibacterial mechanism	Ref.
CDs-LPs	Lactobacillus plantarum	Hydrothermal	Inhibition	*E. coli*	100%	3000	CV + CLSM	Hampering the adhesion process	27
TCDs	Tinidazole	Hydrothermal	Inhibition	*P. gingivalis*	100	150	CV + CLSM + SEM	Hampering the adhesion process	91
N,P-CQDs	Mango peel	Microwave	Inhibition	*E. coli*				Hampering the adhesion process inhibition of quorum sensing	28, and 93
N,F-CQDs	*o*-Phenylenediamine + 2,3,5,6-Tetrafluoroterephthalic acid	Hydrothermal	Inhibition	*E. coli*				Hampering the adhesion process inhibition of quorum sensing	28
C-Dots	Aminoguanidine and citric acid	Hydrothermal	Inhibition	*P. aeruginosa*	50	1000	TEM + CLSM	Inhibition of biofilm formation by killing bacteria	95
CDs	Citric acid and curcumin	Hydrothermal	Inhibition	*S. aureus*					39
				P. aeruginosa	*60*	*500*	CV + CLSM	Inhibition of biofilm formation by killing bacteria	
SPM/DA-CQDs	Polyamines + dopamine	Pyrolysis	Inhibition		80	200	CV	Inhibition of biofilm formation by killing bacteria	96
PL-CD	Poly-lysine	Pyrolysis	Inhibition	*S. aureus*	55	1000	CV + TEM	Inhibition of biofilm formation by killing bacteria	97
CQD_{Lys}	Lysine	Pyrolysis	Inhibition	*S. aureus*	83.1	1000	CV + CLSM + SEM	Inhibition of biofilm formation by killing bacteria	20
CQD_{Arg}	Arginine	Pyrolysis	Inhibition	*S. aureus*	80.1	1000	CV + CLSM + SEM	Inhibition of biofilm formation by killing bacteria	20
Si-QAC CDs	Si-QAC + glycerol	Hydrothermal	Elimination	*S. aureus*	95	500	CV + CLSM	Electrostatic and hydrophobic interactions	98
CQDs	Ethylenediamine + citric acid + ADT-N + $(Alk)_3$	Hydrothermal	Elimination	*S. aureus*	95	64	CV + CLSM	Electrostatic and hydrophobic interactions	43
QCS-EDA-CDs	Chitosan and its derivatives	Hydrothermal	Elimination	*S. aureus*	95	250	CLSM	Hydrophobic interactions	99
Cu-CDs	Citric acid + guanidine hydrochloride + copper chloride	Hydrothermal	Elimination	*S. mutans*	100	240	CLSM	Physical action	100
CD_{600}, CD_{1w}, $CD_{2.5w}$	Citric acid + PEI_{600}/PEI_{10000}/PEI_{25000}	Hydrothermal	Elimination	*S. aureus*	63.9/80.3/97.6	500	CV + CLSM + SEM	Hydrophobic interactions	29
Fe-CDs	Citric acid + $FeSO_4 \cdot 7H_2O$ + ethylenediamine	Hydrothermal	Elimination	*S. aureus*	95	50	CV + CLSM + SEM	ROS	102
FA-CD	Folic acid	Solvothermal	Elimination	*P. aeruginosa* *S. aureus*	82	1000	CV + CLSM + SEM	ROS	63
CQD_{Gent}	Gentamicin sulfate	Pyrolysis	Elimination	*S. aureus*	99	80	CV + CLSM + SEM	Electrostatic interactions ROS	21
GQDs	Carbon fibers	Oxidation cutting	Elimination	*S. aureus*	68	50	SEM	Interfering with the self-assembly of amyloid proteins	103

summarize the antibiofilm mechanisms of carbon dots in Table 2 and discuss them in terms of their inhibitory and destructive effects on biofilms as shown in Scheme 2.

3.1 Inhibition of biofilm formation

Studies have shown that some CDs have inhibitory effects on biofilm formation. Recently, researchers have explained the mechanisms of CDs in the inhibition of biofilm formation.

3.1.1 Hampering the adhesion process. Lin synthesized carbon dots (CDs-LPs) using the biomass of Lactobacillus plantarum.[27] It exhibited no bactericidal activity against *E. coli*, but significantly reduced the colonization and aggregation of *E. coli* on the surface as a way to prevent biofilm formation.[90] FimA, RgpA, RgpB and KGP are the key genes for biofilm formation in *P. gingivalis*. Among them, Fim A plays a key role in the adhesion of gingival porphyrins. As shown in

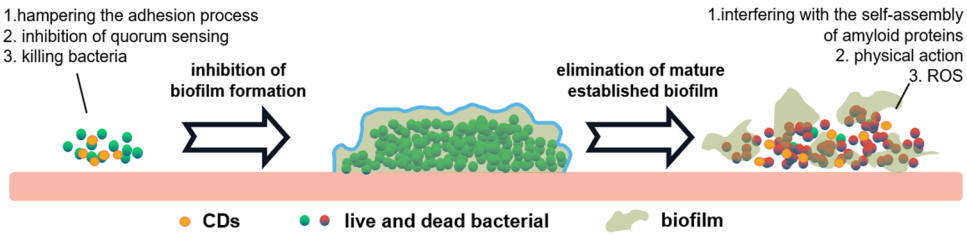

Scheme 2 Antibiofilm mechanism of CDs.

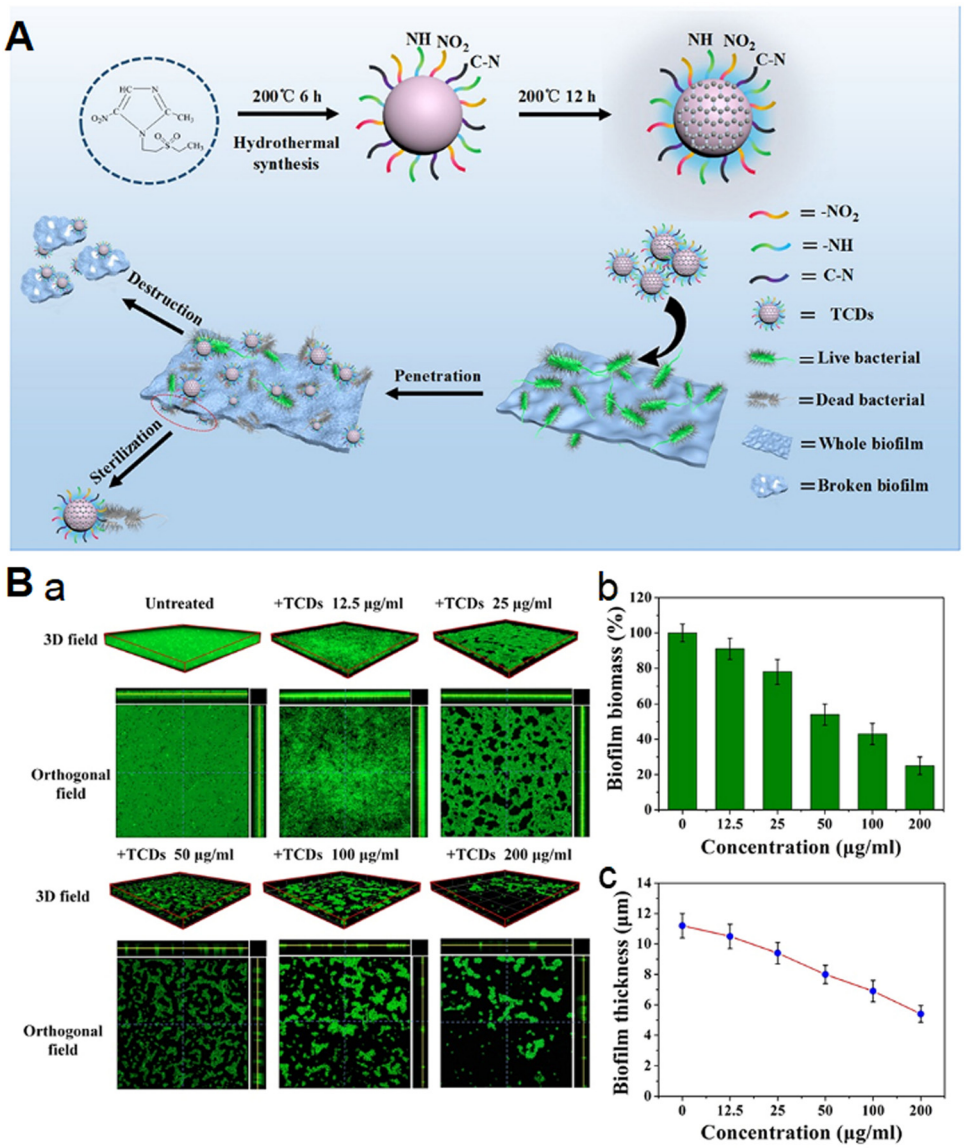

Fig. 9 (A) Schematic of specific antibiofilm activity of carbon quantum dots. (B) Inhibitory effects of TCDs on *P. gingivalis* biofilm formation monitored by CLSM. (a) 3D and orthogonal fields of the inhibitory effects of different concentrations of TCDs on *P. gingivalis* and biofilms by CLSM; (b) the biomass of biofilms after treatments was quantified by FITC fluorescence intensity; (c) biofilm thickness analysis. ''*Int. J. Nanomed.*, 2020, **15**, 5473–5489''[91] Originally published by and used with permission from Dove Medical Press Ltd'.

Fig. 9, Liang *et al.* used a gel assay to detect the mRNA expression of these genes after co-culture with tinidazole carbon dots (TCDs).[91] The results showed that TCDs were able to prevent biofilm formation by inhibiting the gene expression

of biofilm-related genes involved in *P. gingivalis*, thus affecting the self-assembly of biofilm-related proteins. Polysaccharide intercellular adhesin (PIA) is one of the most abundant polysaccharides in the extracellular matrix.[92] It acts as an intercellular adhesin in the aggregation phase of biofilm formation, and its expression directly affects the ability of *S. aureus* biofilm production, while PIA is synthesized by enzyme proteins encoded by the ica operon. Among them, icaA is a transmembrane protein with *N*-acetylphthalate glucosyltransferase activity, which can be regarded as a key gene for the formation of *S. aureus* biofilm. After co-culture of N,P-CQDs and N,F-CQDs prepared by Hua with *S. aureus*, respectively,[28] it was found that the expression level of icaA in *S. aureus* treated with both CQDs was significantly lower than that of the control group. This indicates that both CQDs significantly inhibited the expression of *S. aureus* adhesion-related genes and suppressed its adhesion ability by inhibiting the synthesis of PIA, thus effectively inhibiting the formation of *S. aureus* biofilm.

3.1.2 Inhibition of quorum sensing. The accessory gene regulator (agr) in *S. aureus* is closely related to the regulation of bacterial quorum sensing (QS),[93] which both senses changes in the number of bacterial populations and is a regulator of global

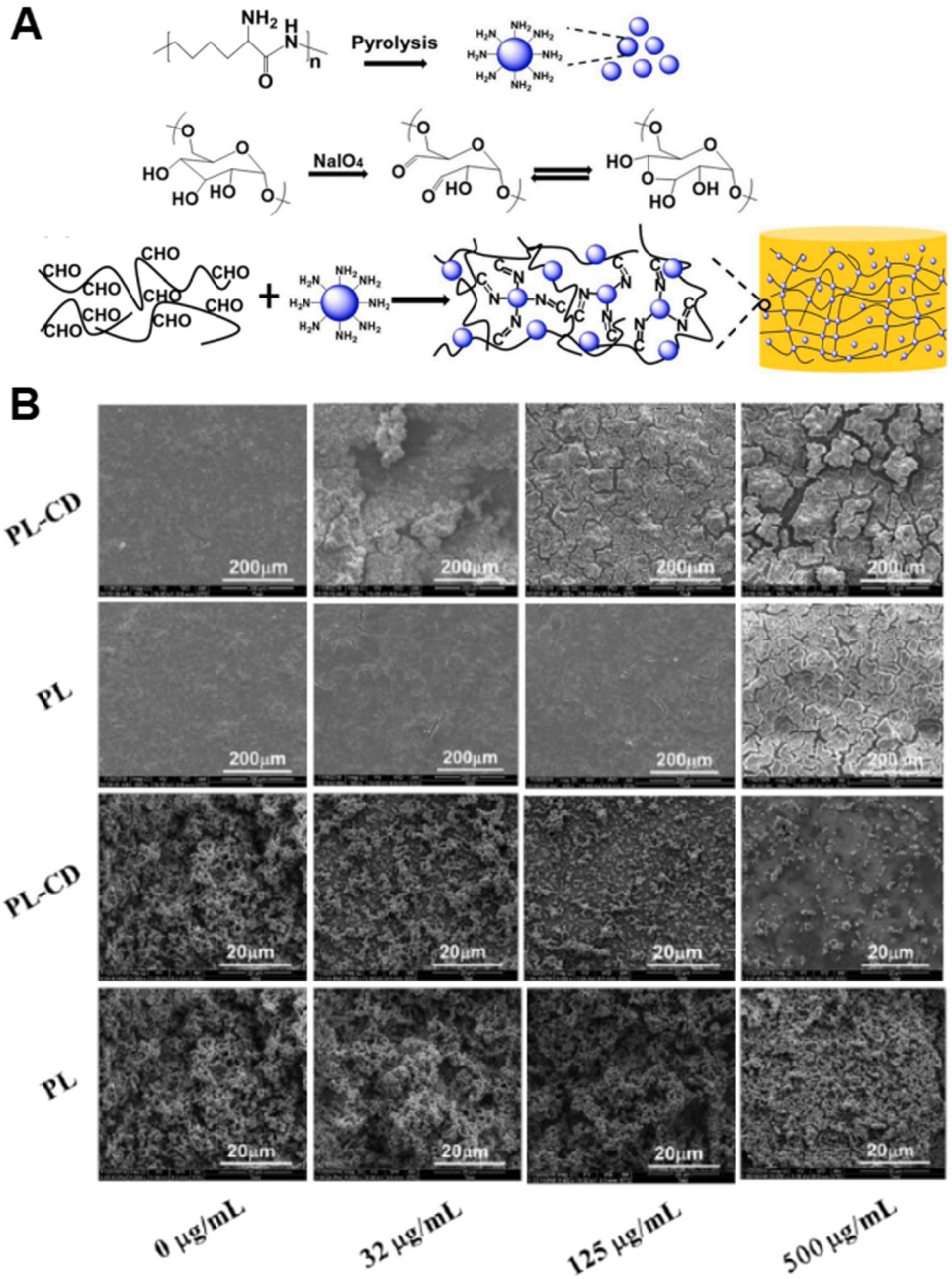

Fig. 10 (A) Preparation of PL-CD, ODA, and PL-CD@ODA hydrogels. (B) Inhibitory effects of PL and PL-CDs on biofilm formation monitored by TEM. Reprinted with permission.[97]

toxin-related proteins. Also, agr plays an important regulatory role in the formation of bacterial biofilms. The expression of pathogenic factors in *S. aureus* invasive infections is mediated by the agr operon, and the agr system can either directly regulate the expression of relevant virulence genes or indirectly by first regulating the expression of other regulators. In Hua's study,[28] the results of RT-PCR assay revealed that the expression of agrA genes was significantly suppressed after the two CQDs entered and interacted with *S. aureus* bacteriophages, which would lead to the suppression of the entire agr quorum sensing regulatory system. Therefore, the two CQDs can be used as a quorum sensing inhibitor to suppress the expression of the agr signaling system and virulence factors of *S. aureus*, inhibiting its quorum sensing and biofilm formation.

3.1.3 Inhibition of biofilm formation by killing bacteria. Biofilms play a protective role for the pairs of bacteria encased in it. However, this self-protective behavior is only associated with surviving bacteria. The CDs prepared by Dong were able to enhance the QS of bacteria after making contact with them,[94] triggering the self-defense response and biofilm formation of bacteria. The growth of biofilm was less in the samples treated with CDs compared to the control. This is because CDs were able to kill most of the bacteria and these behavioral changes were only associated with the surviving bacteria, but they were limited in number and therefore biofilm formation was reduced.

As described in the previous section, CDs can kill bacteria by interacting with them in several ways (*e.g.*, electrostatic interaction, ROS, hydrophobic interaction, *etc.*), which also gives CDs the ability to inhibit biofilm formation. CQDs prepared by Otis *et al.*[95] with aminoguanidine and citric acid could inhibit biofilm formation through the interaction of surface aminoguanidine residues with *P. aeruginosa* lipopolysaccharides. This is because the cationic nature of the surface can facilitate the insertion and penetration of bacterial lipopolysaccharide and phospholipid bilayers to selectively kill *P. aeruginosa*. Lu *et al.*[39] reported that carbon dots prepared with citric acid and curcumin were able to damage bacterial cell membranes by electrostatic action and thus completely inhibit biofilm formation in Gram-negative and Gram-negative bacteria. SPM/DA-CQDs[96] synthesized from a mixture of polyamines (PA) and dopamine (DA) exhibited effective antibiofilm activity and high adhesion on the surface of glass and polymeric contact lens materials as an efficient antibacterial coating. It was able to inhibit the formation of *S. aureus* biofilm effectively by causing bacterial agglutination and disrupting membrane integrity through higher positive charge and surface specific functional groups.

Our group found that CDs prepared with different precursors such as arginine, lysine and poly-lysine were able to inhibit biofilm formation (Fig. 10).[20,97] They were able to kill bacteria through multiple antimicrobial mechanisms, and biofilm formation was significantly reduced with increasing concentrations of CDs.

3.2 Elimination of mature established biofilm

Once a mature biofilm was formed at the site of infection, treating bacterial infection by antibiotics will become extremely difficult. As an ultra-small size antimicrobial agent, CDs can penetrate biofilm more easily than small molecule antibiotics and remove biofilm more completely. Some CDs can remove mature biofilm at the site of infection in the following ways.

3.2.1 Removal of biofilms by physical action. CDs containing long alkyl chain quaternary ammonium groups prepared by Ran *et al.* were able to enter the interior of Gram-positive bacterial biofilms and selectively adsorb to the surface of Gram-positive bacteria through electrostatic and hydrophobic interactions,[98] disrupting the bacterial cell wall/cell membrane and eventually eliminating the biofilm formed by Gram-positive bacteria (Fig. 11). Similarly, Sviridova *et al.*[43] investigated the disruption of Gram-positive *S. aureus* and Gram-negative *E. coli* biofilms by CQDs surface-modified with novel diazonium salts bearing tetraalkylammonium moieties (TAA) of different alkyl chain lengths. The results showed that they could destroy the mature biofilms of *S. aureus* and *E. coli* in a short time and the removal effect appears to be dose dependent. Zhao *et al.*[99] prepared a series of QCS-EDA-CDs using chitosan and its derivatives as precursors with excellent broad-spectrum inhibitory activity against bacterial biofilm formation, especially to *S. aureus* with a minimum inhibitory concentration of 10 $\mu g\ mL^{-1}$. The QCS-EDA-CDs achieve their antimicrobial activity by disrupting the cell membrane and decomposing EPS. Their ultra-small size and hydrophobic organic chains allow them to easily enter the substrate layer of the biofilm, and the abundant quaternary ammonium ions interact with the biofilm to disrupt the matrix structure of the biofilm. In addition, the Cu-doped carbon dots (Cu-CDs) for addressing bacterial biofilm formation, wound infection and dental staining were prepared by Liu *et al.*,[100] which show satisfactory CAT-like activity and were able to effectively remove pathogenic bacterial biofilms by the short-term physical action of oxygen bubbles. The nanoscale Cu-CDs diffused naturally into the mature matrix without any hindrance. In combination with hydrogen peroxide, Cu-CDs were able to completely degrade the EPS matrix, while no significant cell death was induced during the disruption of dense biofilms.

Previously, CDs prepared by our group with different molecular weights of PEI (CQD_{600}, CQD_{1w}, $CQD_{2.5w}$) had a different effect to remove mature biofilms.[29] The reason for this may be that the higher PEI molecular weight results in longer surface chemical groups of the obtained CQDs. The retained hydrophilic PEI layer interacts and fuses with the biofilm and easily inserts into the EPS of the bacterial membrane and penetrates the dense biofilm. The retained PEI molecular chain of the $CQD_{2.5w}$ surface layer is probably the longest, and its disturbance effect on the biofilm is the greatest, thus facilitating the disruption and removal of the mature biofilm.

3.2.2 Biofilm removal by ROS. EPS consists of proteins, polysaccharides and eDNA. eDNA is considered as the "cross-linker" that assembles bacteria and other components of EPS into complete biofilms.[101] eDNA is positively correlated with bacterial adhesion and stability of bacterial biofilms. As shown in Fig. 12, Pan *et al.* assessed the level of residual eDNA within biofilms treated with Fe-CDs by agarose gel electrophoresis.[102]

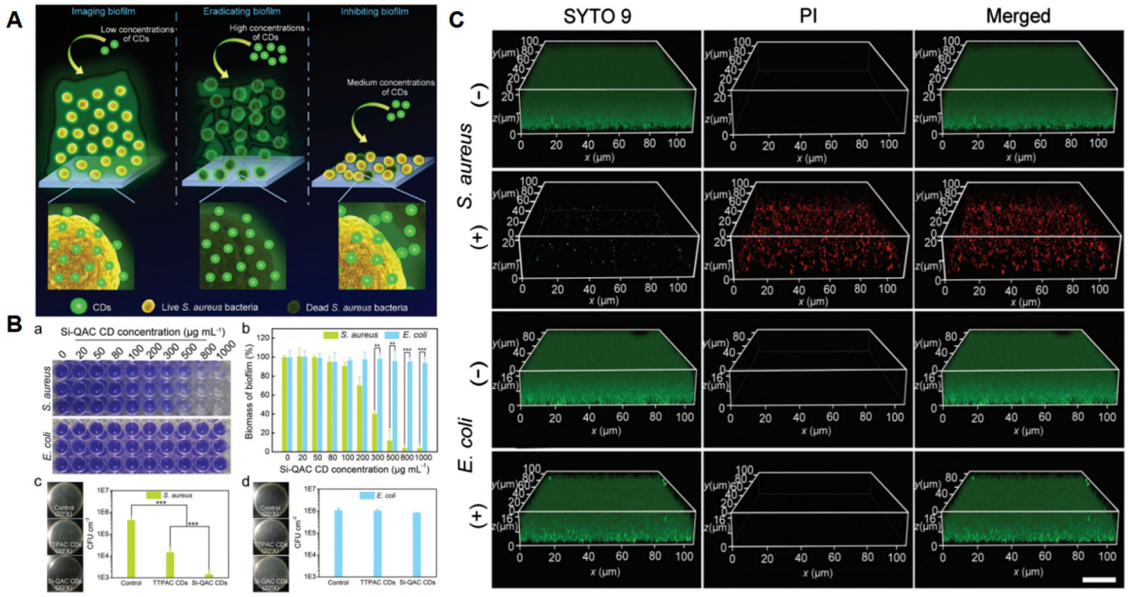

Fig. 11 (A) Schematic illustration of the applications of quaternized CDs for imaging, eradicating and inhibiting *S. aureus* biofilms. (B) Photographs of the CV staining assay results of *S. aureus* and *E. coli* bacterial biofilms after treatment with different concentrations of Si-QAC-CDs for 24 h. (C) 3D confocal fluorescence images of *S. aureus* and *E. coli* biofilms. Reprinted with permission.[98]

The results showed that the residual levels of DNA were significantly lower in biofilms treated with Fe-CDs plus H_2O_2 than in the other groups. The antibiofilm ability of Fe-CDs is mainly attributed to the generation of toxic –OH triggered by a Fenton-like reaction, which allows the effective cleavage of eDNA around the biofilm microenvironment.

Our group found that CQDs prepared with gentamicin had excellent antibiofilm activity at a lower concentration (80 μg mL^{-1}),[21] which readily penetrated biofilms compared with the small molecule gentamicin and killed bacteria in biofilms by multiple mechanisms such as the release of ROS, ultimately leading to the complete destruction of biofilms. FA-CDs recently reported by our group were enriched at the site of infection,[63] and their ultra-small size helped them to enter the biofilm and interact with bacterial cells in the deep biofilm. In the acidic environment of the infection site, FA-CDs can gradually increase intracellular ROS levels, disrupt the ROS homeostasis in bacterial organisms, inactivate a variety of proteins, degrade nucleic acids, and disrupt the integrity of cell membranes, thereby destroying the extracellular polymeric material and thus killing bacteria and removing bacterial biofilms.

3.2.3 Interfering with the self-assembly of amyloid proteins. Amyloid fibers were a key structural component of the extracellular matrix. As shown in Fig. 13, Wang *et al.* synthesized GQDs by a top-down "oxidative cleavage" process.[103] They were capable of mimicking peptide-bound biomolecules and forming supramolecular complexes with phenol-soluble modulins (peptide monomers of amyloid fibrils). The mature

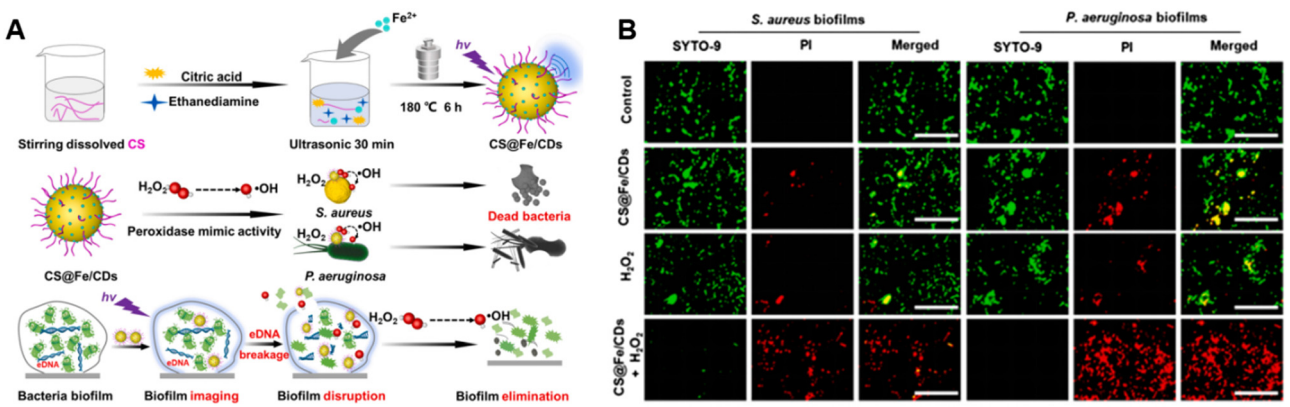

Fig. 12 (A) General design of CS@Fe/CDs-based nanozyme for bacterial biofilm elimination. (B) Bacterial biofilm eradication using CS@Fe/CDs-based nanozyme at 37.0 °C for 3.0 h. Reprinted with permission.[102]

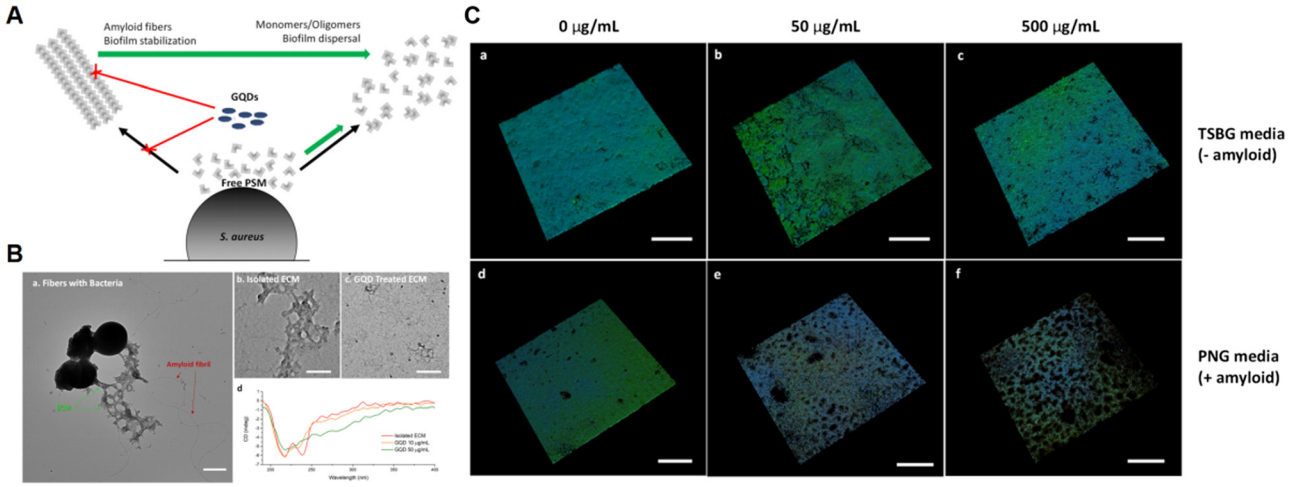

Fig. 13 (A) Schematics of GQD-mediated staphylococcal biofilm dispersal. (B) TEM and CD spectra of isolated ECM from *S. aureus* biofilms grown in PNG and exposed to GQDs. (C) Effects of GQDs on *S. aureus* biofilms. (a–f) Confocal microscopy of *S. aureus* biofilm grown for 3 days and then treated for 1 day. Stains: polysaccharide intercellular adhesin (PIA; green) and bacterial cells (blue). Biofilms grown in TSBG medium in the presence of (a) 0 μg mL^{-1}, (b) 50 μg mL^{-1}, and (c) 500 μg mL^{-1} GQDs. Biofilms grown in PNG medium in the presence of (d) 0 μg mL^{-1}, (e) 50 μg mL^{-1}, and (f) 500 μg mL^{-1} GQDs. Reprinted with permission.[103]

biofilms of *S. aureus* were removed by interfering with the self-assembly of amyloid proteins.

4 Summary and outlook

With excellent antibacterial properties and biocompatibility, CDs are one of the most promising candidates for new generation antimicrobial agents. Compared with antibiotics and other antimicrobial agents, CDs are simple to prepare, less costly, and do not induce bacterial resistance. However, there are still controversies on the antimicrobial mechanism of CDs due to all sorts of reaction conditions and precursors.

To further elucidate the antibacterial and antibiofilm mechanisms of CDs, further theoretical studies are needed. With the researchers' in-depth understanding of their structural features, the photoluminescence mechanism of CDs can be attributed to the surface state, carbon core state, molecular state, and their synergistic effects.[11,34,104–112] This provides inspiration for an in-depth investigation of the antibacterial and antibiofilm mechanisms, and we can use advanced techniques to perform precise structural characterization of the molecular weight, the number of surface groups and the degree of carbonization to reveal the structure–property relationships of CDs.[11,23,34] Meanwhile, gene expression, signaling and other biological process studies should be used to clarify the interaction mode between CDs and bacteria or bacterial biofilms.

In addition, the antibacterial effect of CDs does not originate from a single mechanism only. The antimicrobial effect with multiple mechanisms does not come from the superposition of a single function, and the different mechanisms have synergistic effects with each other, which not only improves the antimicrobial efficiency of CDs and reduces the required bactericidal concentration, but also results in CDs not binding to bacteria completely and specifically in the bactericidal process like antibiotics, avoiding the development of bacterial drug resistance.[20,21,62] Based on this, it is expected that two thorny problems in the antibacterial application of CDs can be solved.

(1) Biocompatibility and antibacterial activity of CDs: although most existing studies support the safe application of CDs, the toxicity profile may vary with the synthesis technique, surface chemistry and testing methods. With in-depth understanding of the antibacterial mechanism of CDs and their structure–performance relationship, we can develop controllable synthesis methods and obtain desirable CDs with both outstanding antibacterial properties and biocompatibility.

(2) Broad-spectrum and narrow-spectrum antibacterial properties of CDs: CDs with broad-spectrum antibacterial properties have a wider range of applications and can be used in different types or complex bacterial infections. However, while broad-spectrum antibacterial agents kill or inhibit the pathogenic bacteria in our body, the beneficial microflora is also broken or inhibited. CDs with selective antibacterial activity have no significant toxicity toward beneficial bacteria and normal cells, reducing the generation of bacterial resistance and side effects in antibacterial therapy. After fully understanding their antibacterial mechanisms, we can prepare CDs according to their required usage.

We hope that this review will serve as a reference for researchers in exploring the antimicrobial mechanisms of CDs and developing novel antibacterial CDs. In the near future, CDs with better antibacterial activity and biocompatibility will be developed as commonly used drugs against bacterial infections in the clinic.

Author contributions

Meizhe Yu was involved in the investigation, formal analysis and writing of the original draft. Peili Li, Ruobing Huang, Chunning Xu, Shiyin Zhang, Yanglei Wang and Xuedong Gong

were involved in the investigation. Xiaodong Xing helped with the conceptualization, funding acquisition, and writing – reviewing and editing.

Conflicts of interest

The authors declare no competing financial interest.

Acknowledgements

This work was supported by a grant from the National Natural Science Foundation of China (81970972).

References

1 P. Krasteva, J. Fong, N. Shikuma, S. Beyhan, M. Navarro, F. Yildiz and H. Sondermann, Vibrio cholerae VpsT regulates matrix production and motility by directly sensing cyclic di-GMP, *Science*, 2010, **327**, 866–868.
2 H. Belt, D. Neut, W. Schenk, J. Horn, H. Mei and H. Staphylococcus, aureus biofifilm formation on different gentamicin-loaded polymethylmethacrylate bone cements, *Biomaterials*, 2001, **22**, 1607–1611.
3 A. S. Utada, R. R. Bennett, J. C. N. Fong, M. L. Gibiansky, F. H. Yildiz, R. Golestanian and G. C. L. Wong, *Nat. Commun.*, 2014, **5**, 4913.
4 J. K. Teschler, D. Zamorano-Sanchez, A. S. Utada, C. J. Warner, G. C. Wong, R. G. Linington and F. H. Yildiz, *Nat. Rev. Microbiol.*, 2015, **13**, 255–268.
5 H. Ji, K. Dong, Z. Yan, C. Ding, Z. Chen, J. Ren and X. Qu, *Small*, 2016, **12**, 6200–6206.
6 J. L. del Pozo and R. Patel, *Clin. Pharmacol. Ther.*, 2007, **82**, 204–209.
7 P. S. Stewart and J. William Costerton, *The Lancet*, 2001, **358**, 135–138.
8 E. Castagnola, F. Bagnasco, A. Mesini, P. K. A. Agyeman, R. A. Ammann, F. Carlesse, M. E. Santolaya de Pablo, A. H. Groll, G. M. Haeusler, T. Lehrnbecher, A. Simon, M. R. D'Amico, A. Duong, E. A. Idelevich, M. Luckowitsch, M. Meli, G. Menna, S. Palmert, G. Russo, M. Sarno, G. Solopova, A. Tondo, Y. Traubici and L. Sung, *Antibiotics*, 2021, **10**, 266.
9 B. Boger, M. Surek, R. O. Vilhena, M. M. Fachi, A. M. Junkert, J. M. Santos, E. L. Domingos, A. F. Cobre, D. R. Momade and R. Pontarolo, *J. Hazard. Mater.*, 2021, **402**, 123448.
10 P. S. Stewart, *Int. J. Med. Microbiol.*, 2002, **292**, 107–113.
11 J. Liu, R. Li and B. Yang, *ACS Cent. Sci.*, 2020, **6**, 2179–2195.
12 C. Xia, S. Zhu, T. Feng, M. Yang and B. Yang, *Adv. Sci.*, 2019, **6**, 1901316.
13 X. Xu, R. Ray, Y. Gu, H. Ploehn, L. Gearheart, K. Raker and W. Scrivens, Electrophoretic Analysis and Purification of Fluorescent Single-Walled Carbon Nanotube Fragments, *J. Am. Chem. Soc.*, 2004, **126**, 12736–12737.
14 L. Wu, X. Li, Y. Ling, C. Huang and N. Jia, *ACS Appl. Mater. Interfaces*, 2017, **9**, 28222–28232.
15 Y. J. Chung, J. Kim and C. B. Park, *ACS Nano*, 2020, **14**, 6470–6497.
16 P. Hou, T. Yang, H. Liu, Y. F. Li and C. Z. Huang, *Nanoscale*, 2017, **9**, 17334–17341.
17 N. Wang, H. Fan, J. Sun, Z. Han, J. Dong and S. Ai, *Carbon*, 2016, **109**, 141–148.
18 H. Zhao, J. Duan, Y. Xiao, G. Tang, C. Wu, Y. Zhang, Z. Liu and W. Xue, *Chem. Mater.*, 2018, **30**, 3438–3453.
19 T. Feng, X. Ai, G. An, P. Yang and Y. Zhao, *ACS Nano*, 2016, **10**, 4410–4420.
20 P. Li, F. Han, W. Cao, G. Zhang, J. Li, J. Zhou, X. Gong, G. Turnbull, W. Shu, L. Xia, B. Fang, X. Xing and B. Li, *Appl. Mater. Today*, 2020, **19**, 100601.
21 P. Li, S. Liu, W. Cao, G. Zhang, X. Yang, X. Gong and X. Xing, *Chem. Commun.*, 2020, **56**, 2316–2319.
22 S. Y. Sung, Y. L. Su, W. Cheng, P. F. Hu, C. S. Chiang, W. T. Chen and S. H. Hu, *Nano Lett.*, 2019, **19**, 69–81.
23 Q. Xin, H. Shah, A. Nawaz, W. Xie, M. Z. Akram, A. Batool, L. Tian, S. U. Jan, R. Boddula, B. Guo, Q. Liu and J. R. Gong, *Adv. Mater.*, 2019, **31**, e1804838.
24 V. Georgakilas, J. A. Perman, J. Tucek and R. Zboril, *Chem. Rev.*, 2015, **115**, 4744–4822.
25 G. Cao, J. Yan, X. Ning, Q. Zhang, Q. Wu, L. Bi, Y. Zhang, Y. Han and J. Guo, *Colloids Surf., B*, 2021, **200**, 111588.
26 T. Mocan, C. T. Matea, T. Pop, O. Mosteanu, A. D. Buzoianu, S. Suciu, C. Puia, C. Zdrehus, C. Iancu and L. Mocan, *Cell. Mol. Life Sci.*, 2017, **74**, 3467–3479.
27 F. Lin, C. Li and Z. Chen, *Front. Microbiol.*, 2018, **9**, 259.
28 J. Hua, *Preparation and Biological Application of Tunable Multicolor Photoluminescent Carbon Dots, MPhil thesis*, Kunming University of Science and Technology, 2019, pp. 82–87.
29 P. Li, X. Yang, X. Zhang, J. Pan, W. Tang, W. Cao, J. Zhou, X. Gong and X. Xing, *J. Mater. Sci.*, 2020, **55**, 16744–16757.
30 X. Wang, K. Qu, B. Xu, J. Ren and X. Qu, *Nano Res.*, 2011, **4**, 908–920.
31 M. Song, Y. Liu, X. Huang, S. Ding, Y. Wang, J. Shen and K. Zhu, *Nat. Microbiol.*, 2020, **5**, 1040–1050.
32 M. C. A. de Oliveira, F. A. G. da Silva, M. M. da Costa, N. Rakov and H. P. de Oliveira, *Adv. Fiber Mater.*, 2020, **2**, 256–264.
33 J. Zhou, Z. Hu, F. Zabihi, Z. Chen and M. Zhu, *Adv. Fiber Mater.*, 2020, **2**, 123–139.
34 L. Ai, Y. Yang, B. Wang, J. Chang, Z. Tang, B. Yang and S. Lu, *Sci. Bull.*, 2021, **66**, 839–856.
35 J. Yang, X. Zhang, Y. H. Ma, G. Gao, X. Chen, H. R. Jia, Y. H. Li, Z. Chen and F. G. Wu, *ACS Appl. Mater. Interfaces*, 2016, **8**, 32170–32181.
36 E. Priyadarshini, K. Rawat, T. Prasad and H. B. Bohidar, *Colloids Surf., B*, 2018, **163**, 355–361.
37 H. J. Jian, R. S. Wu, T. Y. Lin, Y. J. Li, H. J. Lin, S. G. Harroun, J. Y. Lai and C. C. Huang, *ACS Nano*, 2017, **11**, 6703–6716.
38 D. Zhao, Z. Zhang, X. Liu, R. Zhang and X. Xiao, *Mater. Sci. Eng., C*, 2021, **119**, 111468.
39 F. Lu, Y. Ma, H. Wang, M. Zhang, B. Wang, Y. Zhang, H. Huang, F. Liao, Y. Liu and Z. Kang, *Mater. Today Commun.*, 2021, **26**, 102000.

40 F. Cui, J. Sun, J. Ji, X. Yang, K. Wei, H. Xu, Q. Gu, Y. Zhang and X. Sun, *J. Hazard. Mater.*, 2021, **406**, 124330.
41 X. Hao, L. Huang, C. Zhao, S. Chen, W. Lin, Y. Lin, L. Zhang, A. Sun, C. Miao, X. Lin, M. Chen and S. Weng, *Mater. Sci. Eng., C*, 2021, **123**, 111971.
42 J. Yang, G. Gao, X. Zhang, Y.-H. Ma, X. Chen and F.-G. Wu, *Carbon*, 2019, **146**, 827–839.
43 E. Sviridova, A. Barras, A. Addad, E. Plotnikov, A. Di Martino, D. Deresmes, K. Nikiforova, M. Trusova, S. Szunerits, O. Guselnikova, P. Postnikov and R. Boukherroub, *Biomater. Adv.*, 2022, **134**, 112697.
44 L. Hui, J. Huang, G. Chen, Y. Zhu and L. Yang, *ACS Appl. Mater. Interfaces*, 2016, **8**, 20–25.
45 B. Sun, F. Wu, Q. Zhang, X. Chu, Z. Wang, X. Huang, J. Li, C. Yao, N. Zhou and J. Shen, *J. Colloid Interface Sci.*, 2021, **584**, 505–519.
46 N. A. Travlou, D. A. Giannakoudakis, M. Algarra, A. M. Labella, E. Rodríguez-Castellón and T. J. Bandosz, *Carbon*, 2018, **135**, 104–111.
47 H. Sun, N. Gao, K. Dong, J. Ren and X. Qu, *ACS Nano*, 2014, **8**, 6202–6210.
48 S. Tang and J. Zheng, *Adv. Healthcare Mater.*, 2018, **7**, e1701503.
49 J. Huo, Q. Jia, H. Huang, J. Zhang, P. Li, X. Dong and W. Huang, *Chem. Soc. Rev.*, 2021, **50**, 8762–8789.
50 S. Gurunathan, J. W. Han, A. A. Dayem, V. Eppakayala and J. H. Kim, *Int J Nanomedicine*, 2012, **7**, 5901–5914.
51 L. Li, S. Cao, Z. Wu, R. Guo, L. Xie, L. Wang, Y. Tang, Q. Li, X. Luo, L. Ma, C. Cheng and L. Qiu, *Adv. Mater.*, 2022, **34**, e2108646.
52 X. Fan, F. Yang, C. Nie, L. Ma, C. Cheng and R. Haag, *Adv. Mater.*, 2021, **33**, 2100637.
53 X. Fan, X. Wu, F. Yang, L. Wang, K. Ludwig, L. Ma, A. Trampuz, C. Cheng and R. Haag, *Angew. Chem., Int. Ed.*, 2022, **61**, e202113833.
54 Y. Long, L. Li, T. Xu, X. Wu, Y. Gao, J. Huang, C. He, T. Ma, L. Ma, C. Cheng and C. Zhao, *Nat. Commun.*, 2021, **12**, 6143.
55 M. Yu, G. Zhang, P. Li, H. Lu, W. Tang, X. Yang, R. Huang, F. Yu, W. Wu, Y. Xiao and X. Xing, *Mater. Sci. Eng., C*, 2021, **127**, 112225.
56 Z. Gao, D. Yang, Y. Wan and Y. Yang, *Anal. Bioanal. Chem.*, 2020, **412**, 871–880.
57 H.-H. Huang, A. Anand, C.-J. Lin, H.-J. Lin, Y.-W. Lin, S. G. Harroun and C.-C. Huang, *Carbon*, 2021, **174**, 710–722.
58 R. Knoblauch, A. Harvey, E. Ra, K. M. Greenberg, J. Lau, E. Hawkins and C. D. Geddes, *Nanoscale*, 2021, **13**, 85–99.
59 C. Tang, C. Liu, Y. Han, Q. Guo, W. Ouyang, H. Feng, M. Wang and F. Xu, *Adv. Healthcare Mater.*, 2019, **8**, e1801534.
60 Y. Chong, C. Ge, G. Fang, X. Tian, X. Ma, T. Wen, W. G. Wamer, C. Chen, Z. Chai and J. J. Yin, *ACS Nano*, 2016, **10**, 8690–8699.
61 S. Walia, A. K. Shukla, C. Sharma and A. Acharya, *ACS Biomater. Sci. Eng.*, 2019, **5**, 1987–2000.
62 H. Wang, Z. Song, J. Gu, S. Li, Y. Wu and H. Han, *ACS Biomater. Sci. Eng.*, 2019, **5**, 4739–4749.
63 M. Yu, X. Guo, H. Lu, P. Li, R. Huang, C. Xu, X. Gong, Y. Xiao and X. Xing, *Carbon*, 2022, **199**, 395–406.
64 D. Han, Y. Han, J. Li, X. Liu, K. W. K. Yeung, Y. Zheng, Z. Cui, X. Yang, Y. Liang, Z. Li, S. Zhu, X. Yuan, X. Feng, C. Yang and S. Wu, *Appl. Catal., B*, 2020, **261**, 118248.
65 X. Fan, F. Yang, J. Huang, Y. Yang, C. Nie, W. Zhao, L. Ma, C. Cheng, C. Zhao and R. Haag, *Nano Lett.*, 2019, **19**, 5885–5896.
66 B. Geng, Y. Li, J. Hu, Y. Chen, J. Huang, L. Shen, D. Pan and P. Li, *J. Mater. Chem. B*, 2022, **10**, 3357–3365.
67 Y. Liu, B. Xu, M. Lu, S. Li, J. Guo, F. Chen, X. Xiong, Z. Yin, H. Liu and D. Zhou, *Bioactive Mater.*, 2022, **12**, 246–256.
68 Y. Lu, L. Li, M. Li, Z. Lin, L. Wang, Y. Zhang, Q. Yin, H. Xia and G. Han, *Bioconjugate Chem.*, 2018, **29**, 2982–2993.
69 S. Panda, B. ChawPattnayak, P. Dash, B. Nayak and S. Mohapatra, *ACS Appl. Polym. Mater.*, 2021, **4**, 369–380.
70 H. Lu, J. Liu, M. Yu, P. Li, R. Huang, W. Wu, Z. Hu, Y. Xiao, F. Jiang and X. Xing, *Biomater. Sci.*, 2022, **10**, 2692–2705.
71 C. T. McMurray, *Proc. Natl. Acad. Sci. U. S. A.*, 1999, **96**, 1823–1825.
72 M. L. Bochman, K. Paeschke and V. A. Zakian, *Nat. Rev. Genet.*, 2012, **13**, 770–780.
73 D. Svozil, J. Kalina, M. Omelka and B. Schneider, *Nucleic Acids Res.*, 2008, **36**, 3690–3706.
74 S. C. Bera, K. Sanyal, D. Senapati and P. P. Mishra, *J. Phys. Chem. B*, 2016, **120**, 4213–4220.
75 H. Li, J. Huang, Y. Song, M. Zhang, H. Wang, F. Lu, H. Huang, Y. Liu, X. Dai, Z. Gu, Z. Yang, R. Zhou and Z. Kang, *ACS Appl. Mater. Interfaces*, 2018, **10**, 26936–26946.
76 C. Zhao, X. Wang, L. Yu, L. Wu, X. Hao, Q. Liu, L. Lin, Z. Huang, Z. Ruan, S. Weng, A. Liu and X. Lin, *Acta Biomater.*, 2022, **138**, 528–544.
77 H. Wang, M. Zhang, Y. Ma, B. Wang, M. Shao, H. Huang, Y. Liu and Z. Kang, *J. Mater. Chem. B*, 2020, **8**, 2666–2672.
78 J. Chaloupka and V. Vinter, *Folia Microbiol.*, 1996, **41**, 451–464.
79 S. H. Peeters and M. I. de Jonge, *Microbiol. Res.*, 2018, **207**, 161–169.
80 D. J. Dwyer, M. A. Kohanski and J. J. Collins, *Curr. Opin. Microbiol.*, 2009, **12**, 482–489.
81 W. Bing, H. Sun, Z. Yan, J. Ren and X. Qu, *Small*, 2016, **12**, 4713–4718.
82 J. Liu, S. Lu, Q. Tang, K. Zhang, W. Yu, H. Sun and B. Yang, *Nanoscale*, 2017, **9**, 7135–7142.
83 Q. Luo, K. Qin, F. Liu, X. Zheng, Y. Ding, C. Zhang, M. Xu, X. Liu and Y. Wei, *Analyst*, 2021, **146**, 1965–1972.
84 L.-N. Wu, Y.-J. Yang, L.-X. Huang, Y. Zhong, Y. Chen, Y.-R. Gao, L.-Q. Lin, Y. Lei and A.-L. Liu, *Carbon*, 2022, **186**, 452–464.
85 L. S. Wang, A. Gupta and V. M. Rotello, *ACS Infect. Dis.*, 2016, **2**, 3–4.
86 W. M. Dunne, Jr., *Clin. Microbiol. Rev.*, 2002, **15**, 155–166.
87 B. E. Cohen, *Antimicrob. Agents Chemother.*, 2014, **58**, 640–646.

88 B. Thangaraj, P. R. Solomon, S. Chuangchote, N. Wongyao and W. Surareungchai, *ChemBioEng Rev.*, 2021, **8**, 265–301.
89 N. Hoiby, B. Frederiksen and T. Pressler, *J. Cyst. Fibros.*, 2005, **4**(Suppl 2), 49–54.
90 J. Yang, Y. X. Zhu, P. Lu, B. Zhu and F. G. Wu, *J. Mater. Chem. B*, 2022, **10**, 3073–3082.
91 G. Liang, H. Shi, Y. Qi, J. Li, A. Jing, Q. Liu, W. Feng, G. Li and S. Gao, *Int J Nanomedicine*, 2020, **15**, 5473–5489.
92 S. Wu, F. Huang, H. Zhang and L. Lei, *J. Orthop. Surg. Res.*, 2019, **14**, 10.
93 Z. A. Mirani, M. Aziz, M. N. Khan, I. Lal, N. U. Hassan and S. I. Khan, *Microb. Pathog.*, 2013, **61–62**, 66–72.
94 X. Dong, P. Wang, C. E. Rodriguez, Y. Tang, S. Kathariou, Y.-P. Sun and L. Yang, *Mater. Adv.*, 2022, **3**, 6253–6261.
95 G. Otis, S. Bhattacharya, O. Malka, S. Kolusheva, P. Bolel, A. Porgador and R. Jelinek, *ACS Infect. Dis.*, 2019, **5**, 292–302.
96 H.-J. Jian, J. Yu, Y.-J. Li, B. Unnikrishnan, Y.-F. Huang, L.-J. Luo, D. Hui-Kang Ma, S. G. Harroun, H.-T. Chang, H.-J. Lin, J.-Y. Lai and C.-C. Huang, *Chem. Eng. J.*, 2020, **386**, 123913.
97 X. Yang, P. Li, W. Tang, S. Du, M. Yu, H. Lu, H. Tan and X. Xing, *Carbohydr. Polym.*, 2021, **251**, 117040.
98 H. H. Ran, X. Cheng, Y. W. Bao, X. W. Hua, G. Gao, X. Zhang, Y. W. Jiang, Y. X. Zhu and F. G. Wu, *J. Mater. Chem. B*, 2019, **7**, 5104–5114.
99 D. Zhao, R. Zhang, X. Liu, X. Li, M. Xu, X. Huang and X. Xiao, *Int. J. Nanomed.*, 2022, **17**, 937–952.
100 M. Liu, L. Huang, X. Xu, X. Wei, X. Yang, X. Li, B. Wang, Y. Xu, L. Li and Z. Yang, *ACS Nano*, 2022, **16**, 9479–9497.
101 S. Haubenreisser, T. H. Woste, C. Martinez, K. Ishihara and K. Muniz, *Angew. Chem., Int. Ed.*, 2016, **55**, 413–417.
102 T. Pan, H. Chen, X. Gao, Z. Wu, Y. Ye and Y. Shen, *J. Hazard. Mater.*, 2022, **435**, 128996.
103 Y. Wang, U. Kadiyala, Z. Qu, P. Elvati, C. Altheim, N. A. Kotov, A. Violi and J. S. VanEpps, *ACS Nano*, 2019, **13**, 4278–4289.
104 Z. Xie, F. Wang and C. Y. Liu, *Adv. Mater.*, 2012, **24**, 1716–1721.
105 J. Yu, X. Yong, Z. Tang, B. Yang and S. Lu, *J. Phys. Chem. Lett.*, 2021, **12**, 7671–7687.
106 B. Yuan, Z. Xie, P. Chen and S. Zhou, *J. Mater. Chem. C*, 2018, **6**, 5957–5963.
107 Z. Han, Y. Ni, J. Ren, W. Zhang, Y. Wang, Z. Xie, S. Zhou and S. F. Yu, *Nanoscale*, 2019, **11**, 11577–11583.
108 J. Wang, S. Zhang, Y. Li, C. Wu, W. Zhang, H. Zhang, Z. Xie and S. Zhou, *Small*, 2022, **18**, e2203152.
109 H. Chen, B. Wang, D. Gao, M. Guan, L. Zheng, H. Ouyang, Z. Chai, Y. Zhao and W. Feng, *Small*, 2013, **9**, 2735–2746.
110 X. Dong, Y. Wang, R. Guan, J. Ren and Z. Xie, *Small*, 2021, **17**, e2105273.
111 T. Chao, X. Dong, J. Wang, R. Song, Z. Xie and S. Zhou, *ACS Appl. Nano Mater.*, 2022, **5**, 15720–15727.
112 F. Wang, Z. Xie, H. Zhang, C.-Y. Liu and Y.-G. Zhang, *Adv. Funct. Mater.*, 2011, **21**, 1027–1031.

